



All Theses and Dissertations

2016-03-01

Forward Chemical Genetics Drug Screen Yields Novel Proteases and Proteolytic Inhibitors of HGF–induced Epithelial–Mesenchymal Transition

Jeffrey Thomas Schuler
Brigham Young University

Follow this and additional works at: <https://scholarsarchive.byu.edu/etd>

 Part of the [Physiology Commons](#)

BYU ScholarsArchive Citation

Schuler, Jeffrey Thomas, "Forward Chemical Genetics Drug Screen Yields Novel Proteases and Proteolytic Inhibitors of HGF–induced Epithelial–Mesenchymal Transition" (2016). *All Theses and Dissertations*. 6257.
<https://scholarsarchive.byu.edu/etd/6257>

This Thesis is brought to you for free and open access by BYU ScholarsArchive. It has been accepted for inclusion in All Theses and Dissertations by an authorized administrator of BYU ScholarsArchive. For more information, please contact scholarsarchive@byu.edu, ellen_amatangelo@byu.edu.

Forward Chemical Genetics Drug Screen Yields Novel Proteases and Proteolytic Inhibitors
of HGF-induced Epithelial-Mesenchymal Transition

Jeffrey Thomas Schuler

A thesis submitted to the faculty of
Brigham Young University
in partial fulfillment of the requirements of the degree of
Master of Science

Marc D. Hansen, Chair
Juan A. Arroyo
Joshua L. Andersen

Department of Physiology and Developmental Biology

Brigham Young University

March 2016

Copyright © 2016 Jeffrey Thomas Schuler

All Rights Reserved

ABSTRACT

Forward Chemical Genetics Drug Screen Yields Novel Proteases and Proteolytic Inhibitors of HGF-induced Epithelial-Mesenchymal Transition

Jeffrey Thomas Schuler

Department of Physiology and Developmental Biology, BYU
Master of Science

Hepatocyte Growth Factor (HGF)-induced Epithelial-Mesenchymal Transition (EMT) is a complex cellular pathway that causes epithelial cell scattering by breaking cell-cell contacts, eliminating apical-basal polarity, and replacing epithelial markers and characteristics with mesenchymal markers. Early EMT events include a brief period of cell spreading, followed by cell compaction and cell-cell contact breaks. A forward chemical genetics drug screen of 50,000 unique compounds measuring HGF-induced cell scattering identified 26 novel EMT inhibitors, including 2 proteolytic inhibitors. Here, we show that B5500-4, one of the EMT inhibitors from the screen, blocks HGF-induced EMT by a predicted blocking of the protease furin, in addition to secondarily blocking Beta-Secretase (BACE).

We also show that MMP-12 and MMP-9 are required for HGF-induced EMT to progress. MMP-12 is required for cell contraction, and its inhibition produces a continuous cell spreading phenotype.

We also demonstrate that both furin and BACE activity are required for HGF-induced EMT to proceed, but that they are involved in separate pathways. We show that BACE inhibition leads to a failure of cell spreading in early EMT, and that EphA2 is a member of this pathway. We also demonstrate that it is likely BACE2, and not BACE1 that is responsible for early cell spreading. Furin is also required for HGF-induced cell scattering, but does not play a role in the cell spreading process. These findings highlight the importance of proteolytic activity at the earliest stages of HGF-induced EMT.

Key Words: EMT, cell spreading, cell compaction, HGF, BACE, EphA2, Furin, MMP-9, MMP-12

ACKNOWLEDGEMENTS

I would like to deeply, deeply thank my research advisor, Dr. Marc Hansen. In the spring of 2010, I entered his office to learn more about his lab and research. While he provided answers to my questions, we ended up talking more about hockey, Minnesota, and movies. That meeting—while at the time seeming so inconsequential—set me on the path to devoting myself to the study and science of physiology and cell biology, to pursuing this master's degree, and to ultimately altering my life and career goals for the better. I am forever grateful to Dr. Hansen for his mentorship, guidance, friendship, and patience.

I also acknowledge the pillar of support and love that my family has been to me, not just through my time as a graduate student, but through my whole life. To my sisters and brother, my grandparents, my two nephews, and especially to my loving parents, I say thank you. Thank you for helping me to become who I am today.

I would like to thank the other members of my graduate committee, Dr. Juan Arroyo and Dr. Joshua Andersen, for their guidance and help through my graduate student journey. I have always felt kindness and support from each of you as I have stepped and stumbled my way through my degree. Thank you.

I also thank Jessica Jensen and Melissa McNeil for their help with cell culture and live cell imaging. They were invaluable assets to me. Also to Dr. Watt and Catalina Rodriguez, who were instrumental in providing molecular docking data on B5500-4. Thanks are also in order for Frost Biologic, who provided key data to the characterization of B5500-4.

I express my deepest thanks and gratitude to the Department of Physiology and Developmental Biology for funding me through TA and RA opportunities. This work would not have been possible otherwise.

I would also like to take a moment to thank Connie Provost for her constant guidance and help through the entire graduate school process, from applying, to scheduling, to filling out forms and paperwork, and to getting me towards graduating. Thank you so much for your constant prodding to get me in the right direction. It was always a pleasure to work with you.

TABLE OF CONTENTS

TITLE PAGE.....	i
ABSTRACT.....	ii
ACKNOWLEDGEMENTS.....	iii
TABLE OF CONTENTS.....	iv
LIST OF FIGURES.....	vi
CHAPTER 1: Introduction and Literature Review.....	1
An Overview of the Biological Uses of Epithelial-Mesenchymal Transition.....	1
The Role of EMT in Disease Progression.....	2
The Role of HGF and the c-Met Pathway in Driving the EMT Program.....	3
The Role of Proteases in EMT and HGF-pathway Programs.....	5
A High-Throughput EMT Assay Yields Novel EMT Inhibitors.....	5
CHAPTER 2: Results.....	7
HGF Causes Cell Surface Area Spreading, then Contraction in MDCK Cells.....	7
Identification and Chemical Optimization of B5500.....	8
B5500-4 Target Identification.....	10
The Functional Requirement of MMPs in HGF-induced Epithelial Cell Scattering.....	12
BACE is Required for Epithelial Cell Spreading in Early HGF-induced EMT; Furin is Required for Epithelial Cell Scattering, but Not Y-secretase.....	13
Summary of Novel Proteases Involved in HGF-pathway.....	14
CHAPTER 3: Discussion.....	15
Cellular Mechanics of Early EMT.....	15

B5500-4 Characteristics and Mechanism.....	16
MMP Function in the Mechanics of HGF-induced Epithelial Scattering.....	17
Furin and BACE in HGF-induced Epithelial Cell Scattering.....	18
CHAPTER 4: Methods and Protocols.....	19
Immunofluorescence Assay.....	19
EMT Migration Assay.....	19
SW71 Cell Invasion Assay.....	19
Time-lapse Live Cell Microscopy.....	20
Western Blot	20
qPCR Array.....	21
GLISA Assay.....	22
REFERENCES.....	23
CURRICULUM VITAE.....	39

LIST OF FIGURES

Figure 2.1: HGF-induced EMT Includes Phase of Cell Spreading, Followed by Phase of Cell Contraction.....	28
Figure 2.2: Characterization and Optimization of B5500.....	29
Figure 2.3: Inflammation Assay Reveals No Significant Change in Inflammatory Marker Expression	30
Figure 2.4: Kinase Screen of B5500 Does Not Block Kinases in Kinase Screen.....	31
Figure 2.4 (continued): Kinase Screen of B5500 Does Not Block Kinases in Kinase Screen.....	32
Figure 2.5: B5500-4 Does Not Alter Levels of Classic EMT Markers.....	33
Figure 2.6: qPCR Array Results Indicate Fold-increase of Select Genes.....	34
Figure 2.7: MMP-9 is Required for HGF-induced Epithelial Cell Scattering, and MMP-12 is Required for HGF-induced Cell Contraction Phase of Epithelial Cell Scattering.....	35
Figure 2.8: Furin Inhibition Blocks HGF-induced EMT; Y-Sec Inhibition is Cytotoxic.....	36
Figure 2.9: BACE is Required for Early EMT Cell Spreading.....	37
Figure 2.10: Model for Proteolytic Activity during Early EMT Events.....	38

CHAPTER 1: Introduction and Literature Review

An Overview of the Biological Uses of Epithelial-Mesenchymal Transition

The development of most organ systems requires restructuring and reorganization of embryonic cells into functional tissues through multiple stages of Epithelial-mesenchymal transition (EMT) and mesenchymal-epithelial transition (MET) (Birchmeier 1996). Groups of individual cells assemble into epithelial tissues by forming cell-cell contacts with their neighbors and establishing an apical-basal polarity, which occurs through the sequential organization of adherens junctions, tight junctions, and desmosomes (Barasch 2001). Additionally, gap junctions between cells enable communication throughout the epithelial cell layer (Defamie 2014). Separation between epithelial sheets and adjacent tissues is maintained by the formation of a basal lamina, a layer of extracellular matrix upon which epithelial sheets sit (Barasch 2001). Mesenchymal cells, on the other hand, maintain minimal cell-cell contacts, invade through and within the extracellular matrix, and are typically found throughout connective tissues below the epithelial layer and its basal lamina (Defamie 2014).

The transformation from epithelial to mesenchymal phenotype is a complex cellular event characterized by the loss of cell-cell junctions and apical-basal polarity, and the acquisition of mesenchymal characteristics and migratory abilities (Stoker 1985, Weidner 1991, Bhargava 1992, Ridley 1995). Epithelial cells are induced to undergo EMT, or 'scatter' in the case of cultured cells, by a variety of signaling and environmental factors, including HGF, VEGF, EGF, TGF-beta, Wnt, Notch, tissue wounding, and hypoxia (Ridley 1995, Morabito 2001, Kim 2002, Timmerman 2004, Saika 2003, Boyer 1992). EMT is induced by these different factors at

some of the earliest stages of tissue organization during embryonic development (Kalcheim 2015).

Three distinct stages of EMT and MET are required for determining the final cell-fates of many specialized tissues, and are referred to as Primary, Secondary, and Tertiary EMT. The first instances of EMT within the developing embryo are known as Primary EMT, and occur in most multicellular organismal development (Kalcheim 2015). Examples include EMT events during mammalian implantation, during gastrulation in metazoans, and during neural crest development in vertebrates. The formation of the parietal endoderm is one of the first EMT events in embryonic development. Cells from the inner cell mass break cell-cell contacts, migrate through the primitive endoderm, and relocate along the inner blastocyst walls to form the parietal endoderm (Kalcheim 2015). Mesoderm formation also requires EMT. In this process cells invade through the primary streak and reorganize into the mesodermal tissue. EMT is also observed throughout later development. Somites undergo EMT during the vertebral development of the embryo. Several rounds of EMT and MET occur during heart valve development (Barasch 2001).

The Role of EMT in Disease Progression

While epithelial cell scattering is required for embryonic development, tissue maintenance, and wound healing, its inappropriate activation contributes pathologically to fibrosis, Crohn's disease, cataract formation, and cancer metastasis (Bataille 2008, Kalluri 2003, de Longh 2005, Ruiz 1996).

Cancer and some other disease types misuse EMT to form dangerous and life-threatening phenotypes. Cancer cells often hijack EMT pathways, leading to increased cell

scattering and mesenchymal characteristics. Cancer cells undergoing EMT produce proteolytic enzymes that degrade the basement membrane, allowing for individual cells to locally invade and migrate to distant tissues. Mesenchymal-epithelial transition then occurs, resulting in the formation of distant metastases (Polyak 2009). Accompanying EMT during cancer progression are a variety of changes to cellular behavior, including resistance to apoptosis, enhanced survival, genome instability, and resistance to chemotherapy, all of which affect disease progression and prognosis (Blick 2008, Kalluri 2009, Polyak 2009). It is particularly important to figure out the best methods of inhibiting the EMT program from progressing in cancer, as metastatic cancer is much more difficult to treat than non-metastatic cancer.

The Role of HGF and the c-Met Pathway in Driving the EMT Program

Hepatocyte Growth Factor (HGF) and its target, the c-Met receptor tyrosine kinase are of particular interest in cancer research. HGF-induced EMT initiates a complex and specific program referred to as invasive growth, and is most often characterized by the dissociation of cell-cell junctions via decreased membrane-localized E-cadherin, and increased N-cadherin expression. Downstream activation of the RAS, PI3K, STAT, Notch, and beta-catenin signaling pathways are required for HGF-induced EMT to progress (O'Brien 2004, Marshall 1995, Graziani 1991, Boccaccio 1998, Monga 2002). The switch from epithelial to mesenchymal states is driven by activation of key transcription factors SNAIL, SLUG, TWIST, and ZEB1/2 (Rodriguez-Paredes 2011). In carcinomas, aberrant activation of the c-Met pathway leads to more metastatic behavior in cancers and to a poorer prognosis in multiple cancer types (Baschnagel 2014, Yoshinao 2000, Masuya 2004).

Epigenetic changes can also regulate EMT progression. Cell scattering can be initiated when mesenchymal genes and their promoter sites undergo H3 acetylation or H3K4 trimethylation, or when there is hypermethylation of their repressor sites (Rodriguez-Paredes 2011, Ehrlich 2009, Ehrlich 2002). The miRNA-200 and miRNA-205 families have specifically been linked to the regulation of the EMT program, which in turn are regulated by histone modification (Fullgrabe 2011). These and many other epigenetic factors have shown pronounced effects in the regulation of the cell scattering program.

In addition to intracellular signaling cascades and regulatory networks, a variety of extracellular environmental cues contribute to the HGF-induced cell scattering event. Cell-substrate stiffness can directly influence the ability of epithelial cells to undergo HGF-induced EMT (Hoj 2014); increasing the pliability of the surface substratum reduces cell-substrate tension, which in turn reduces HGF-induced cell scattering (Hoj 2014). Increases in cell-substrate tension also leads to increased nuclear localization of YAP/TAZ, which act as mechanotransduction sensors and mediators that respond to tension changes in the cellular microenvironment (Sirio 2011).

Other signaling pathways can also interact with and affect the progression of HGF-induced cell scattering. TGF-beta can enhance HGF-induced EMT, and has a chemotaxic effect on scattering cells. VEGF and TGF-beta act competitively to enhance HGF, and VEGF will neutralize the additive scattering of TGF-beta (Chung 2011). The crosstalk that exists between major signaling pathways and the c-Met pathway serves to underscore the complexity of the scattering pathway, and emphasizes the need to further study this cellular event in greater detail.

The Role of Proteases in EMT and HGF-pathway Programs

Among the earliest changes in cell behavior during EMT initiation includes proteolytic activation and deactivation (Tervonen 2015, Craig 2015, Ha 2015, Gray 2014). Cell surface serine protease Hepsin activity increases downregulates HGF activator inhibitor type 1 (HAI-1), increasing HGF-pathway activation and EMT progression (Tervonen 2015). Chemical inhibition of matrix metalloproteinases 2/9 by Sorafineb inhibits c-Met and MEK/ERK pathways, leading to decreased migration and invasion of hepatocellular carcinoma cells (Ha 2015). Additionally, matrix metalloproteinases 3, 7, and 8 have been implicated in EMT progression in patients with idiopathic pulmonary fibrosis (Craig 2015). Additionally, type-II transmembrane serine protease matriptase inhibition leads to a failure of HGF-dependent EMT in MDCK cells (Gray 2014).

Increasing numbers of proteases are being found to regulate EMT progression; however, the roles of many of these proteases have yet to be fully understood (Tervonen 2015). Additionally, many additional proteases may yet hold undiscovered roles in c-Met pathway and EMT regulation.

A High-Throughput EMT Assay Yields Novel EMT Inhibitors

While traditional research methods have provided valuable insights into signaling pathways and their mechanics, a forward chemical genetics screen provides a fresh perspective of the c-Met pathway by allowing for the simultaneous discovery of novel molecular components and new drug inhibitors of HGF-induced EMT. Pharmacologically inhibiting the scattering phenotype not only provides the opportunity to further understand the molecular components of the pathways involved, but can also reveal the therapeutic potential and clinical relevance of the novel inhibitors in the treatment of several human diseases,

including and especially cancer metastasis (Kubinyi 2002, Russel 2004, Carlson 2012, Cornelius 2011) .

The forward chemical genetic screen stands as a unique method for identifying novel molecular components in a pathway, and provides several key advantages and disadvantages. In this approach, molecules from large chemical libraries are assessed for biological activity in a high-throughput and high content assay system that measures the biological output of some cellular process or pathway. Compounds identified in screening are expected to target cellular machinery required for the cellular process or pathway of interest. The drawback to this method is that once a drug candidate is identified, further work must be done to identify the molecular target of the compound.

In a prior publication, we reported a drug screen of 50,000 distinct chemical compounds in a high throughput assay testing inhibition of cell scattering and reported those with known biological activity, which highlights how this approach works (Langford 2012). In our screening assay, MDCK cells are seeded on a 96-well trans-well plate and induced to undergo EMT with HGF. The screen yielded 20 biologically relevant small chemical inhibitors of HGF-induced cell scattering out of the compound library. One of these 20 chemical scaffolds is a neuronal calcium channel blocker (Langford 2012). Subsequent experiments designed to understand why a calcium channel blocker would prevent EMT revealed that a calcium influx follows HGF stimulation and is required for progression of EMT.

CHAPTER 2: Results

HGF Causes Cell Surface Area Spreading, then Contraction in MDCK Cells

The cellular events associated with HGF-induced epithelial scattering of MDCK cells have been carefully characterized previously (Sperry 2010). Here we repeat the results of Sperry et al. (Sperry 2010) by seeding MDCK cells into collagen-coated imaging dishes. After 24-48 hours, small colonies of MDCK cells were picked for brightfield live cell imaging before initiation of imaging. To observe epithelial scattering, cultures were stimulated with HGF immediately prior to initiation of imaging. For each experiment, we performed imaging on a minimum of 15 colonies in order that we might observe reproducible effects throughout each culture. Further, experiments were reproduced 3 times to highlight any differences between independent experiments. Thus, for each experimental condition, we analyzed at least 3x colonies of MDCK cells. Our results show that MDCK cell colonies stimulated with HGF undergo cell spreading, which occurs within the first two hours after HGF treatment (Fig. 2.1A). To quantitatively define this cell spreading, we measured the amount of the culture dish covered by colonies of MDCK cells during imaging and normalized this area to the number of cells in each colony. This quantitation shows that MDCK cell contact with the collagen substrate increases by some 44% within the first two hours (Fig. 2.1A, C). Following the two hour cell spreading phase, HGF-induced MDCK cell colonies begin a period of contraction that lasts the following 6 hours. During contraction, cells initiate migration and rupture cell-cell adhesions. According to our quantitation of cell area during imaging, MDCK cell surface area returns to levels observed prior to responding to HGF stimulation and may contract even further, particularly as cell-cell contacts break. Unstimulated MDCK cells show limited changes in cell spreading, not

contractile activity, limited migration, and only slow repositioning within the colony (Fig. 2.1B). While we do see unstimulated colonies grow in size, there is no net gain in cell area as most of the change in size is accounted for by cell division.

Identification and Chemical Optimization of B5500

From the 50,000 chemical compound pilot screen, 20 biologically active EMT blockers were identified, including one nicotinamide derivative, N-(5-iodo-6-methyl-2-pyridinyl)-3-nitrobenzamide (B5500) (Fig. 2.2A). Of these, 11 bear an unknown mechanism of action.

We reasoned that molecules of high interest would affect cellular machinery required for EMT in multiple model systems, so we sought to assess which molecules might affect EMT in another system unrelated to MDCK cells. Further, the ability to use human cell lines, as opposed to canine MDCK cells, would allow us to employ a number of assay systems that rely on human cell lines and that could provide key information about the molecular target of our compounds. We therefore assessed compounds that are active in our screening assay for the activity in blocking invasive behavior of the trophoblast cell line Sw71. Screening these 11 compounds through a cell invasion assay of SW71 human trophoblast cells in a collagen matrix again demonstrated their ability to block EMT from progressing, demonstrating a molecular mechanism that is present in multiple organism and tissue types (in this case, canine kidney and human trophoblast cell lines) (Fig. 2.2C). Of the 11 EMT inhibitors tested in the SW71 invasion assay, 7 compounds showing statistically significant reduction of invasion, including B5500. 10 μ M B5500 inhibited SW71 invasion by 33% of the DMSO control trial.

We sought to determine which of these molecules would be the most likely to reveal novel biology about epithelial scattering. One issue with our overall approach is that

microtubules are required for epithelial scattering of MDCK cells in response to HGF. Since microtubule-targeting agents are found with high frequency in phenotypic assays, we sought to avoid working with compounds that inhibit HGF-induced EMT by targeting the microtubule cytoskeleton. In order to understand which molecules target microtubules, we assessed compounds from our original screen in proliferation assays using the NCI-60 panel of cancer cell lines. Since microtubules are required for cell division, compounds bearing microtubule targeting activity would inhibit cell proliferation of the majority of cell lines in this panel. Inhibition of a subset of cell lines would instead suggest the targeting of a protein required for the growth of some cells, revealing a potential mechanism of action for the compound under question. We found that only B5500 had no general effects on cell growth in these proliferation assays, meaning it is the only compound that certainly works independently of a microtubule-based mechanism.

We sought to optimize the specific activity of B5500 in arresting HGF-induced epithelial scattering. We generated 49 chemical derivatives of B5500 and assessed them in our original screening assay, yielding three analogs with increased activity (Fig. 2.2D). For each of these new derivatives, the activity in affecting scattering or migration was compared to anti-proliferative activity. B5500-25 and B5500-26 show potent cell growth inhibition that accompanies their activity in the HGF-induced EMT assay. Another compound, N-(5-bromo-6-methyl-2-pyridinyl)-pyrimidine-5-carboxamide (B5500-4) (Fig. 2.2B), affects cell proliferation only at high concentrations, but retains significant activity in blocking HGF-induced EMT. This compound likely affects HGF-induced EMT completely independently of microtubules. Since it is

more potent than B5500, we sought to use this molecule for our subsequent target identification experiments.

In order to confirm that B5500-4 affects scattering behavior of human cells and to determine its potency, we measured its activity in invasion assays using SW71 cells at decreasing concentrations. We found that B5500-4 does in fact block EMT and invasion in this system and does so with an IC-50 of ~27 nM (Fig. 2.2B).

B5500-4 Target Identification

We initially sought to identify a target pathway for B5500 and B5500-4 by assessing the readout of compound treatment in a series of cell culture systems in which inflammatory biomarker expression is analyzed. This so-called BIO-Map system consists of primary human cells that are grown in culture alone or in combination, then activated to generate an inflammatory response. In total, 12 different culture models were used and expression of a total of >70 inflammatory markers were analyzed. The value of this system is that inhibition of a signaling pathway will give a predictable readout that will be comparable to that generated with inhibitors of known pathway components. As such, the BIO-Map system is a powerful approach to identifying the target of a small molecule inhibitor of unknown mechanism, at least at the pathway level. However, no significant changes in the expression of any inflammatory markers were associated with B5500-4 treatment in this system (Fig. 2.3), suggesting that this molecule does not target signal transduction machinery.

Additionally, B5500 was assessed for its activity in blocking the activity of protein kinases with a panel of 230 kinases. B5500 was not active against any kinases tested (Fig. 2.4).

This compound is not a kinase inhibitor, as we might expect from the lack of a discernable readout in the BIO-Map system.

To determine what effects B5500-4 had on more classic EMT markers, we performed western blots on e-Cadherin (E-cad), SNAIL, and SLUG in several human cancer cell lines (A549, Psn-1, and Panc-1). A549, a human lung cancer cell line, maintains many epithelial characteristics, including high expression of E-cad, and low expression of mesenchymal markers SNAIL and SLUG. Interestingly, the B5500-4-treated cell lines show no statistically significant change in E-cad, SNAIL, or SLUG protein levels in cancer cell lines A549, Psn-1, and Panc-1 (Fig. 2.5A). This finding suggests that B5500-4 does not act by increasing epithelial characteristics within cells (A549), nor by decreasing mesenchymal characteristics (Psn-1, Panc-1). This does not rule out, however, that B5500-4 could act via preventing the transition from epithelial to mesenchymal states.

In order to identify any changes in gene expression caused by B5500-4, we performed a qPCR assay of 384 genes known to be involved in the regulation of EMT, extracellular matrix, cytoskeleton (Fig. 2.6A-D). SW71 cell samples were induced with B5500-4 or DMSO (control) for 24 hours, and cDNA samples were produced from harvested mRNA extracts. The cDNA samples were run through the PCR plates, and the differential expression of various genes in cells treated with B5500-4 or DMSO compared. Several genes demonstrated large changes in expression with B5500-4 treatment, including and especially Col4A2 (1.05×10^4 fold change), MMP-12 (-7.37×10^6 fold change), and mTOR (-2.22×10^3 fold change) (Fig. 2.6A-B).

The Functional Requirement of MMPs in HGF-induced Epithelial Cell Scattering

The changes in expression of MMP-12 and of extracellular matrix in cells treated with B5500-4 suggest a possible role for cell surface proteases in the HGF pathway. The chemical structure of B5500-4 is also suggestive of binding within a proteolytic binding pocket, as the central amide bond of the linker region closely resembles the peptide bond of an amino acid chain (Fig. 2.2B). We hypothesized that B5500-4 might be a protease inhibitor and specifically target proteases in the MMP family. MMPs have already been implicated in EMT progression and cancer metastasis, but the roles of MMP-12 and MMP-9 have yet to be fully characterized in the context of epithelial cell scattering, cell spreading, and cell contraction (Craig 2015, Ha 2015).

In order to determine whether matrix metalloproteinases are required for HGF-induced EMT, inhibitors of proteases MMP-12 and MMP-9 were used to treat MDCK cells prior to induction of scattering with HGF.

Chemical inhibition of MMP-9 by Ilomastat of HGF-induced MDCK cells blocks EMT (Fig. 2.7C). Neither cell spreading nor cell compaction occurs (Fig. 2.7E), indicating an unknown role for MMP9 within the c-Met cell scattering program. It is possible that MMP9 is required for both cellular processes, or that its role precedes cell spreading and contraction.

MDCK cells treated with Marimastat (a blocker of MMP-12) fail to scatter after HGF stimulation (Fig. 2.7). While spreading is observed, it is drastically slowed. MDCK colonies treated with Marimastat take 8 hours to reach the extent of maximal spreading observed in control MDCK cells, which occurs in 2 hours (Fig. 2.7E). Additionally, no cell compaction is observed for the duration of the experiment. This suggests that MMP-12 must be required

for activation of the cell compaction program, but it remains unclear how MMP-12 inhibition alters the time-frame and rate of cell spreading.

BACE is Required for Epithelial Cell Spreading in Early HGF-induced EMT; Furin is Required for Epithelial Cell Scattering, but Not Y-secretase

We sought to test whether B5500 or B5500-4 are inhibitors of matrix metalloproteinases. Biochemical assays measuring the activity of different MMPs were performed in the presence of a series of concentration of B5500. We tested several MMP family members, including MMP 1-3, 7-10, and 12-14. None of these proteases demonstrated any reduction in activity at even the highest concentration (10 μ M) of B5500. Despite that MMPs are indeed required for HGF-induced epithelial scattering of MDCK cells, B5500 does not prevent scattering by targeting MMPs.

In order to test whether the molecular target(s) of B5500-4 included any other proteases during EMT, a collaborator conducted molecular modeling experiment to measure B5500-4 binding affinity cell surface proteases (furin and beta-secretase (BACE)). In both cases, B5500-4 was expected to bind the active site of these proteases. We therefore determined to test the role of these proteases in HGF-induced epithelial scattering.

MDCK cells were seeded onto collagen-coated imaging plates, treated with appropriate inhibitor, stimulated to undergo epithelial scattering with HGF treatment, and subjected to live cell imaging (Fig. 2.8). Darunavir (furin chemical inhibitor) treatment resulted in a failure of epithelial cell scattering, suggesting a role for furin in the HGF pathway (Fig. 2.8A). Neither cell spreading nor cell contraction occurs in furin-inhibited MDCK cells during HGF stimulation, especially when compared with HGF-control MDCK cells (Fig. 2.1).

Chemical inhibition of Y-secretase proved to be cytotoxic; cell die 6 hours after treatment (Fig. 2.8B), suggesting an important survival role for Y-secretase, one that acts independently of the c-Met pathway.

MDCK cells treated with BACE inhibitor fail to undergo normal HGF-induced scattering. These cells showed undergo a cell compaction without undergoing any cell spreading. No effect of BACE inhibitor is observed in MDCK cells that have not been stimulated with HGF (Fig. 2.9A-B). The compaction observed in BACE-treated cells parallels cell compaction in control cells treated with HGF after spreading has occurred (Fig. 2.9B). These results suggest a role for BACE in the HGF pathway through regulating cell spreading, but not in cell compaction.

Summary of Novel Proteases Involved in HGF-pathway

An illustration provides a graphical summary of the roles of the tested proteases within the c-Met pathway (Fig. 2.10). When induced with HGF, MDCK cells begin a cell spreading phase, which requires BACE. After 2 hours of spreading, the MDCK cells undergo a cell contraction phase, which requires MMP12. Regulation of both of these processes likely requires MMP9 and furin, but not Y-secretase, which activity is likely required for cell survival.

CHAPTER 3: Discussion

Cellular Mechanics of Early EMT

Consistent with earlier reports, we have shown that MDCK cells undergo HGF-induced epithelial cell scattering in a two-phase process, beginning with an early phase of cell spreading and followed by a later cell contraction phase. It is during the cell contraction phase that cell-cell contacts are broken and cells fully separate from their neighbors, allowing for formerly epithelial cells to migrate and invade as individual, solitary mesenchymal cells.

Whether cell-cell contacts become weakened during early epithelial scattering, such as during the early cell spreading phase, remains an open question. The current thinking of the field, though in flux, is that forces coming from migration or other actomyosin-based contractile processes are sufficient to rupture fully cell-cell junctions without any prior changes to the molecular architecture of the junction. In support of this, it appears that reduction in and restoration of cellular contractility is enough to rupture cell-cell contacts (Hoj 2014), indicating that contractile forces alone are enough to rupture cell-cell junctions. However, our prior work show that exogenous expression of a 'constitutively active' fragment of the cytoskeleton-membrane linker protein, zyxin, results in an inability of cells to detach from each other during epithelial scattering and results in cells that attempt to migrate while maintaining long tethers to other cells (Sperry 2011). A resolution to this controversy is that contractile forces are likely sufficient to drive cell-cell detachment during HGF-induced epithelial scattering, but that this must be preceded by a relaxation of actomyosin-based tension forces that results in uncoupling of cadherin cell-cell adhesion receptors from the actin binding protein, alpha-catenin, which

form cadherin-catenin-actin complexes that link cell contacts to the actin cytoskeleton only when under tension.

Our focus here has been to study and characterize the mechanics of this two phase process. A powerful approach to understanding complex cellular processes in tissue culture models, particularly for identifying cellular components required for the process under question, is to employ unbiased chemical screening. We follow up on a high content phenotypic screening approach that led us to a molecule with activity that is highly specific for blocking HGF-induced epithelial scattering and not cell division processes (a sign of microtubule targeting).

B5500-4 Characteristics and Mechanism

We optimized the original molecule identified in screening to increase the specificity for inhibition of HGF-induced epithelial scattering over anti-proliferative activity, yielding the molecule B5500-4. This molecule inhibits HGF-induced epithelial scattering in MDCK cells in the original screening assay and blocks invasion of trophoblast cells with high potency. Interestingly, it produces no effect on the expression of classic EMT markers, such as E- and N-cadherin, SLUG, and SNAIL, when used to treat mesenchymal cancer cells. While we have not looked at whether B5500-4 can prevent expression of mesenchymal markers in cells undergoing epithelial scattering, our results suggest that inhibition of the target of our compound cannot induce a reversion to an epithelial phenotype among cells that are already mesenchymal.

Defining the mechanism of action of B5500 and B5500-4 has proven to be a major challenge, as is often the case for molecules identified in phenotypic high content screens.

Assessment for activity in blocking the activity of a large panel of 230 kinases shows that these compounds are not kinase inhibitors. We then turned to another high content screen where inhibition of different signaling pathways has specific and recognizable readout patterns, the so-called BioMAP screen. Even here the results are negative and suggest that the target of these compounds is not a signaling molecule.

Clues to the identity of the molecular target were first obtained in assessing changes in expression patterns resulting from B5500-4 treatment using a PCR array system, where the most affected genes are an extracellular matrix protein and a matrix metalloproteinase. In fact, recent findings from this lab have shown that characteristics of the extracellular matrix, including its substrate stiffness, can have dramatic effects on the ability of MDCK cells to migrate while undergoing HGF induction (Hoj 2014) and support a role for matrix remodeling enzymes like MMPs in HGF-induced epithelial scattering.

MMP Function in the Mechanics of HGF-induced Epithelial Scattering

The MMP proteins MMP-12 and MMP-9 had both been shown in previous studies to be involved in epithelial cell scattering, though not directly in response to HGF [40]. While our qPCR assay indicates that MMP-12 might be a target of B5500-4 and is thus required for epithelial cell scattering, we also assessed other MMP proteins for which there are readily available inhibitors. Our time-lapse microscopy of epithelial scattering of MDCK cells in the presence of Marimastat and Ilomastat, chemical inhibitors of MMP-12 and MMP-9, respectively, demonstrates that MMP-9 and -12 are both required for epithelial cell scattering in MDCK cells. More interesting is that MMP-12 inhibition blocked the cell contraction phase without affecting the cell spreading phase. MMP-9, in contrast, inhibited both cell spreading

and cell contraction phases of the cell scattering program, suggesting a molecular target upstream and required for both programs in the scattering pathway.

Furin and BACE in HGF-induced Epithelial Cell Scattering

While MMP-9 and -12 were shown to be required for epithelial scattering, biochemical assays reveal that B5500 is not an inhibitor of matrix metalloproteinases. Clues as to its mechanism came from docking studies performed by a collaborator in silico and suggested that B5500 and B5500-4 bind the active sites of the surface proteases furin and BACE. To our knowledge, a role for either protease in HGF-induced epithelial scattering has not been reported. BACE is produced as an inactive proenzyme protease and requires proteolytic processing to become an active BACE protease (Creemers 2001). Interestingly, it is furin that has been reported to mediate BACE processing (Creemers 2001). Treating MDCK cells with inhibitors of these proteases and examining the impact of epithelial scattering reveals that both are required, though the effect of inhibition of each protease is distinct. And since furin is one of the major proteases to convert pro-BACE to BACE, it was assumed that both would be involved in the same pathway. The findings that BACE inhibition causes an HGF-dependent cell contraction response in MDCK cells, whereas furin does not, went against our hypothesis. We had hypothesized that the inhibition of either protease would produce a similar cellular effect, and yet it was the opposite that proved true. It became apparent that while furin may be responsible for pro-BACE cleavage, this certainly wasn't the method of BACE activation involved in the c-Met pathway.

CHAPTER 4: Methods and Protocols

Immunofluorescence Assays

Showing alterations to actin rearrangement via Frost-100 were demonstrated using immunofluorescence assays. MDCK cells plated for 24-hours onto collagen-coated coverslips were induced with HGF and either B5500-4, B5500, or DMSO (control). After a 24 hour incubation period, cells were fixed via paraformaldehyde, and stained with phalloidin, anti-BACE, or anti-EphA2 for subsequent imaging.

EMT Migration Assays

EMT assays were performed to quantify the anti-scattering effects of B5500 and B5500-4. MDCK cells were plated onto trans-well plates and left to incubate for 24 hours. At 24 hours, the cells were induced with both HGF and either B5500-4, B5500, or DMSO (control) at a variety of concentrations (10 μ M, 1 μ M, 0.1 μ M, 0.01 μ M) and given an additional 24 hours to migrate through the membrane. Cells were fixed via paraformaldehyde, and stained with crystal violet stain. Fixed cells on the upper membrane surface were wiped away with cotton swabbing, leaving only migrated cells on the bottom of the transwell filter membrane. The wells were imaged and quantified using the SpotDenso tool on the Fluorchem Analysis program.

SW71 Cell Invasion Assay

The invasion assay measures the amount of cellular invasion colonies of cells undergo, which in part relies on the ability of the cells to undergo EMT. Matrigel solution was poured into a bottom well of a transmembrane system, on top of a thin-film membrane and allowed time to congeal. SW71 cells were seeded into the plate's top chamber and starved of Fetal Bovine Serum (FBS). A FBS gradient was created by adding a 5% FBS solution in the bottom

well. The FBS acted as a chemoattractant to the FBS-starved cells, initiating invasion down through the matrigel. B5500-4 and B5500 were added at increasing concentrations (10 μ M, 1 μ M, 0.1 μ M, 0.01 μ M) to the top well at the same time as the introduction of the FBS gradient. A 24 hour incubation period was allowed for the cells to invade. Cells were then fixed and stained with a Dissociation solution, and the bottom membrane was extracted and used to generate a cell count for the invaded cells.

Time-lapse Live-cell Microscopy

MDCK cells seeded onto collagen-coated Delta-T movie dishes for 24 hours will be induced with Frost-100 at 10 μ M, followed shortly by HGF. Single-frame images will be taken at multiple time points (every 2 minutes for 13 hours) and stitched together into a time-lapse movie using Slidebook software. Comparing Frost-100 induced MDCK cells to DMSO control MDCK cells will reveal the effects that Frost-100 have on inhibiting migratory behavior.

Western Blot

Western blot of classic EMT protein markers--E-cadherin, N-cadherin, Slug, and Snail--were performed to quantify the changes to the epithelial state of the target cells induced with Frost-100. MDCK cells were seeded for 24 hours and subsequently induced with HGF and increasing concentrations of B5500-4 or B5500 (10 μ M, 1 μ M, 0.1 μ M, 0.01 μ M). At 24 hours after induction, cells were lysed using a cell lysis buffer containing 2-mercaptoethanol and protease inhibitors, and the cytosolic contents were collected and isolated via centrifugation. A Bradford assay was performed on each of the cell lysate samples to equalize relative protein concentrations, which was run through an SDS-PAGE gel, and transferred to a nitrocellulose membrane. The membrane was incubated with either anti-e-cadherin antibodies, anti-n-

cadherin antibodies, anti-Slug antibodies, or anti-Snail primary antibodies followed by secondary antibodies. Final blot images were then developed using the enhanced chemiluminescence (ECL) detection system. The same membranes were also developed in an anti- β -actin primary antibody (mouse), followed by anti-mouse secondary antibodies in a subsequent blot to provide an internal control. Quantification of the blots were obtained using the spot-denso analysis tool on the developed X-ray films as a part of the Fluorchem SP imaging system.

qPCR Array

Human trophoblast SW71 cells were cultured for 24 hours and then induced with 5 μ M B5500-4 or with DMSO (control). After an additional 24 hour incubation time, the cells were harvested and the RNA extracted using a Qiagen RNA extraction kit. The RNA samples were equalized via Nanodrop spectrophotometry, and reverse-transcribed into cDNA using the Invitrogen Superscript II Reverse Transcriptase kit. The cDNA was added to SYBR Mastermix, aliquotted into the PCR array plate, and run through a Qiagen thermocycler for 50 cycles, according to kit specifications. The Frost-100 and DMSO cDNA samples were compared to each other in terms of number of cycles needed to reach an arbitrary threshold, which assigned each trial a raw score, and gave an indication to the relative amounts of RNA from each sample and the fold-change between the two samples. Individual genes with the highest fold-change in expression were repeated in multiplicates to confirm the change in expression.

GLISA Assay

A specific type of ELISA assay—the GLISA assay—was performed to measure ATP-bound proteins of interest, showing the effects of B5500-4 on the levels of the specific proteins in their activation state. SW71 cells were seeded for 24 hours and subsequently induced with B5500-4 at a variety of concentrations (10 μ M, 1 μ M, 0.1 μ M, 0.01 μ M) for an additional 24 hours. Cells were harvested with a cell lysis buffer containing 2-mercaptoethanol and protease inhibitors, centrifuged, and snap frozen in liquid nitrogen. Equalized protein samples—measured via Bradford assay—were then added to each well containing the GLISA substrates. After incubation for 1 hour, lysate contents were discarded, and primary antibody solution was added and allowed to incubate for 30 minutes. Primary antibody solution was discarded and replaced with a secondary antibody solution, and incubated for 1 hour. The wells were rinsed and fixing reagent was added and allowed to incubate for 15 minutes. The freezing reagent was added and the wells are imaged and quantified using spectrophotometry.

REFERENCES

- Barasch J. Genes and proteins involved in mesenchymal to epithelial transition. *Curr Opin Nephrol Hypertens*. 2001 May;10(3):429-36. Review.
- Baschnagel AM, Williams L, Hanna A, Chen PY, Krauss DJ, Pruetz BL, Akervall J, Wilson GD. c-Met expression is a marker of poor prognosis in patients with locally advanced head and neck squamous cell carcinoma treated with chemoradiation. *Int J Radiat Oncol Biol Phys*. 2014 Mar 1;88(3):701-7. doi: 10.1016/j.ijrobp.2013.11.013.
- Basso D, Bozzato D, Padoan A, Moz S, Zambon CF, Fogar P, Greco E, Scorzeto M, Simonato F, Navaglia F, Fassan M, Pelloso M, Dupont S, Pedrazzoli S, Fassina A, Plebani M. Inflammation and pancreatic cancer: molecular and functional interactions between S100A8, S100A9, NT-S100A8 and TGF β 1. *Cell Commun Signal*. 2014 Mar 26;12:20. doi: 10.1186/1478-811X-12-20.
- Bataille F, Rohrmeier C, Bates R, Weber A, Rieder F, Brenmoehl J, Strauch U, Farkas S, Fürst A, Hofstädter F, Schölmerich J, Herfarth H, Rogler G. Evidence for a role of epithelial mesenchymal transition during pathogenesis of fistulae in Crohn's disease. *Inflamm Bowel Dis*. 2008 Nov;14(11):1514-27. doi: 10.1002/ibd.20590.
- Bhargava M, Joseph A, Knesel J, Halaban R, Li Y, Pang S, Goldberg I, Setter E, Donovan MA, Zarnegar R, et al. Scatter factor and hepatocyte growth factor: activities, properties, and mechanism. *Cell Growth Differ*. 1992 Jan;3(1):11-20.
- Birchmeier C1, Birchmeier W, Brand-Saberi B. Epithelial-mesenchymal transitions in cancer progression. *Acta Anat (Basel)*. 1996;156(3):217-26
- Boccaccio C, Andò M, Tamagnone L, Bardelli A, Michieli P, Battistini C, Comoglio PM. January 1998. "Induction of epithelial tubules by growth factor HGF depends on the STAT pathway". *Nature* 391 (6664): 285–8. doi:10.1038/34657.
- Boyer MJ, Tannock IF. Regulation of intracellular pH in tumor cell lines: influence of microenvironmental conditions. *Cancer Res*. 1992 Aug 15;52(16):4441-7.
- Carlson SM, White FM. Expanding applications of chemical genetics in signal transduction. *Cell Cycle* 2012; 11:1903 - 1909; PMID: 22544320.
- Chung JY, Davis JA, Price BD, Staley DM, Wagner MV, Warner SL, Bearss DJ, Hansen MD. Competitive enhancement of HGF-induced epithelial scattering by accessory growth factors. *Exp Cell Res*. 2011 Feb 1;317(3):307-18. doi: 10.1016/j.yexcr.2010.11.002.
- Cornelius J. O'Connor, Luca Laraia and David R. Spring. Tutorial Review Chemical genetics. *Chem. Soc. Rev.*, 2011,40, 4332-4345 DOI: 10.1039/C1CS15053G

- Craig VJ, Zhang L, Hagood JS, Owen CA. Matrix metalloproteinases as therapeutic targets for idiopathic pulmonary fibrosis. *Am J Respir Cell Mol Biol*. 2015 Nov;53(5):585-600. doi: 10.1165/rcmb.2015-0020TR. Review.
- Creemers JW, Ines Dominguez D, Plets E, Serneels L, Taylor NA, Multhaup G, Craessaerts K, Annaert W, De Strooper B. Processing of beta-secretase by furin and other members of the proprotein convertase family. *J Biol Chem*. 2001 Feb 9;276(6):4211-7. Epub 2000 Nov 8.
- de Longh R.U. Wederell E. Lovicu F.J. McAvoy J.W. Transforming Growth Factor- β -Induced Epithelial-Mesenchymal Transition in the Lens: A Model for Cataract Formation. *Cells Tissues Organs* 2005;179:43–55 (DOI:10.1159/000084508)
- Defamie N, Chepied A, Mesnil M. Connexins, gap junctions and tissue invasion. *FEBS Lett*. 2014 Apr 17;588(8):1331-8. doi: 10.1016/j.febslet.2014.01.012. Epub 2014 Jan 20. Review.
- Di Renzo MF1, Olivero M, Giacomini A, Porte H, Chastre E, Mirossay L, Nordlinger B, Bretti S, Bottardi S, Giordano S, et al. Overexpression and amplification of the met/HGF receptor gene during the progression of colorectal cancer. *Clin Cancer Res*. 1995 Feb;1(2):147-54.
- Ehrlich M. DNA hypomethylation in cancer cells. *Epigenomics*. 2009;1:239–259.
- Ehrlich M. DNA methylation in cancer: too much, but also too little. *Oncogene*. 2002;21:5400–5413.
- Fischer OM, Giordano S, Comoglio PM, Ullrich A. Reactive oxygen species mediate Met receptor transactivation by G protein-coupled receptors and the epidermal growth factor receptor in human carcinoma cells. *J Biol Chem*. 2004 Jul 9;279(28):28970-8.
- Fullgrabe J, Kavanagh E, Joseph B. Histone onco-modifications. *Oncogene*. 2011;30:3391–3403.
- Gray K, Elghadban S, Thongyoo P, Owen KA, Szabo R, Bugge TH, Tate EW, Leatherbarrow RJ, Ellis V1. Potent and specific inhibition of the biological activity of the type-II transmembrane serine protease matriptase by the cyclic microprotein MCoTI-II. *Thromb Haemost*. 2014 Aug;112(2):402-11. doi: 10.1160/TH13-11-0895. Epub 2014 Apr 3.
- Graziani A, Gramaglia D, Cantley LC, Comoglio PM. November 1991. "The tyrosine-phosphorylated hepatocyte growth factor/scatter factor receptor associates with phosphatidylinositol 3-kinase". *J. Biol. Chem*. 266 (33): 22087–90.
- Gude NA, Emmanuel G, Wu W, Cottage CT, Fischer K, Quijada P, Muraski JA, Alvarez R, Rubio M, Schaefer E, Sussman MA (May 2008). "Activation of Notch-mediated protective signaling in the myocardium". *Circ. Res*. 102(9): 1025–35.doi:10.1161/CIRCRESAHA.107. 164749.

- Ha TY, Hwang S, Moon KM, Won YJ, Song GW, Kim N, Tak E, Ryoo BY, Hong HN. Sorafenib inhibits migration and invasion of hepatocellular carcinoma cells through suppression of matrix metalloproteinase expression. *Anticancer Res.* 2015 Apr;35(4):1967-76.
- Hoj JP, Davis JA, Fullmer KE, Morrell DJ, Saguibo NE, Schuler JT, Tuttle KJ, Hansen MD. Cellular contractility changes are sufficient to drive epithelial scattering. *Exp Cell Res.* 2014 Apr 26. pii: S0014-4827(14)00169-4. doi: 10.1016/j.yexcr.2014.04.011.
- Kalchauer C. Epithelial-Mesenchymal Transitions during Neural Crest and Somite Development. *J Clin Med.* 2015 Dec 25;5(1). pii: E1. doi: 10.3390/jcm5010001. Review.
- Kalluri R, EG Neilson. Epithelial-mesenchymal transition and its implications for fibrosis. *J Clin Invest.* 2003;112(12):1776–1784. doi:10.1172/JCI20530.
- Kim K, Lu Z, Hay ED. Direct evidence for a role of beta-catenin/LEF-1 signaling pathway in induction of EMT. *Cell Biol Int.* 2002;26(5):463-76.
- Kubinyi H, Weinmann H, Jaroch S.. Chemogenomics in drug discovery. Chemical genomics small molecule probes to study cellular function. Berlin: Springer. ISBN 3-540-27865-6.
- Kusunoki H, Taniyama Y, Otsu R, Rakugi H, Morishita R. Anti-inflammatory effects of hepatocyte growth factor on the vicious cycle of macrophages and adipocytes. *Hypertens Res.* 2014 Mar 13. doi: 10.1038/hr.2014.41. PMID: 24621470.
- Langford PR, L Keyes, and MDH Hansen. Plasma membrane ion fluxes and NFAT-dependent gene transcription contribute to c-met-induced epithelial scattering. *J Cell Sci* 125, 4001-4013. Sep 2012. doi: 10.1242/jcs.098269.
- Marshall CJ. January 1995. "Specificity of receptor tyrosine kinase signaling: transient versus sustained extracellular signal-regulated kinase activation". *Cell* 80 (2): 179–85. doi:10.1016/0092-8674(95)90401-8.
- Masuya D, C Huang, D Liu, T Nakashima, K Kameyama, R Haba, M Ueno and H Yokomise. The tumour–stromal interaction between intratumoral c-Met and stromal hepatocyte growth factor associated with tumour growth and prognosis in non-small-cell lung cancer patients. *British Journal of Cancer* (2004) 90, 1555–1562. doi:10.1038/sj.bjc.6601718
- Monga SP, Mars WM, Padiaditakis P, Bell A, Mulé K, Bowen WC, Wang X, Zarnegar R, Michalopoulos GK. April 2002. "Hepatocyte growth factor induces Wnt-independent nuclear translocation of beta-catenin after Met-beta-catenin dissociation in hepatocytes". *Cancer Res* 7 (62): 2064–71. ISSN 0008-5472.

- Morabito CJ, Dettman RW, Kattan J, Collier JM, Bristow J. Positive and negative regulation of epicardial-mesenchymal transformation during avian heart development. *Dev Biol.* 2001 Jun 1;234(1):204-15.
- Miura K, Nam JM, Kojima C, Mochizuki N, Sabe H. EphA2 engages Git1 to suppress Arf6 activity modulating epithelial cell-cell contacts. *Mol Biol Cell.* 2009 Apr;20(7):1949-59. doi: 10.1091/mbc.E08-06-0549. Epub 2009 Feb 4.
- Murakami K, Kuniyoshi K, Iwakura N, Matsuura Y, Suzuki T, Takahashi K, Ohtori S. Vein Wrapping for Chronic Nerve Constriction Injury in a Rat Model: Study Showing Increases in VEGF and HGF Production and Prevention of Pain-Associated Behaviors and Nerve Damage. *J Bone Joint Surg Am.* 2014 May 21;96(10):859-67. doi: 10.2106/JBJS.L.01790.
- O'Brien LE, Tang K, Kats ES, Schutz-Geschwender A, Lipschutz JH, Mostov KE. July 2004. "ERK and MMPs sequentially regulate distinct stages of epithelial tubule development". *Dev. Cell* 7 (1): 21–32. doi:10.1016/j.devcel.2004.06.001.
- Polyak, K. and R. A. Weinberg. "Transitions between epithelial and mesenchymal states: acquisition of malignant and stem cell traits." *Nat Rev Cancer* (2009) 9(4):265-273.
- Ridley AJ, Comoglio PM, Hall A. Regulation of scatter factor/hepatocyte growth factor responses by Ras, Rac, and Rho in MDCK cells. *Mol Cell Biol.* 1995 Feb;15(2):1110-22.
- Rodriguez-Paredes M, Esteller M. Cancer epigenetics reaches mainstream oncology. *Nat Med.*2011;17:330–339.
- Ruiz P, Günthert U. The Cellular Basis of Metastasis. *World J Urol.* 1996;14(3):141-50.
- Russel K, Michne WF (2004). "The value of chemical genetics in drug discovery". In Folkers G, Kubinyi H, Müller G, Mannhold R. *Chemogenomics in drug discovery: a medicinal chemistry perspective.* Weinheim: Wiley-VCH. pp. 69–96. ISBN 3-527-30987-X.
- Saika S, Miyamoto T, Tanaka S, Tanaka T, Ishida I, Ohnishi Y, Ooshima A, Ishiwata T, Asano G, Chikama T, Shiraishi A, Liu CY, Kao CW, Kao WW. Response of lens epithelial cells to injury: role of lumican in epithelial-mesenchymal transition. *Invest Ophthalmol Vis Sci.* 2003 May;44(5):2094-102.
- Saito T, Yoshida K, Matsumoto K, Saeki K, Tanaka Y, Ong SM, Sasaki N, Nishimura R, Nakagawa T. Inflammatory cytokines induce a reduction in E-cadherin expression and morphological changes in MDCK cells. *Res Vet Sci.* 2014 Apr;96(2):288-91. doi: 10.1016/j.rvsc.2014.02.005.
- Sirio Dupont, Leonardo Morsut, Mariaceleste Aragona, Elena Enzo, Stefano Giulitti, Michelangelo Cordenonsi, Francesca Zanconato, Jimmy Le Digabel, Mattia Forcato, Silvio

- Bicciato, Nicola Elvassore & Stefano Piccolo. Role of YAP/TAZ in mechanotransduction. *Nature* 474,179–183 (09 June 2011) doi:10.1038/nature10137.
- Sperry RB, Bishop NH, Bramwell JJ, Brodeur MN, Carter MJ, Fowler BT, Lewis ZB, Maxfield SD, Staley DM, Vellinga RM, Hansen MD. Zyxin controls migration in epithelial-mesenchymal transition by mediating actin-membrane linkages at cell-cell junctions. *J Cell Physiol.* 2010 Mar;222(3):612-24. doi: 10.1002/jcp.21977.
- Stoker M, M. Perryman. An epithelial scatter factor released by embryo fibroblasts. *J. Cell Sci.*, 77 (1985), pp. 209–223.
- Tania M, Khan MA, Fu J. Epithelial to mesenchymal transition inducing transcription factors and metastatic cancer. *Tumour Biol.* 2014 Jun 2. PMID:24880591.
- Tervonen TA, Belitškin D, Pant SM, Englund JI, Marques E, Ala-Hongisto H, Nevalaita L, Sihto H, Heikkilä P, Leidenius M, Hewitson K, Ramachandra M, Moilanen A, Joensuu H, Kovanen PE, Poso A, Klefström J. Deregulated hepsin protease activity confers oncogenicity by concomitantly augmenting HGF/MET signalling and disrupting epithelial cohesion. *Oncogene.* 2015 Jul 13. doi: 10.1038/onc.2015.248.
- Timmerman LA, Grego-Bessa J, Raya A, Bertrán E, Pérez-Pomares JM, Díez J, Aranda S, Palomo S, McCormick F, Izpisua-Belmonte JC, de la Pompa JL. Notch promotes epithelial-mesenchymal transition during cardiac development and oncogenic transformation. *Genes Dev.* 2004 Jan 1;18(1):99-115. Epub 2003 Dec 30.
- Weidner KM, Arakaki N, Hartmann G, Vandekerckhove J, Weingart S, Rieder H, Fonatsch C, Tsubouchi H, Hishida T, Daikuhara Y, et al. Evidence for the identity of human scatter factor and human hepatocyte growth factor. *Proc Natl Acad Sci U S A.* 1991 Aug 15;88(16):7001-5.
- MD Yoshinao O.D.A., MD Akio Sakamoto, MD Tsuyoshi Saito, Naoko Kinukawa, MD Yukihide Iwamoto, MD Masazumi Tsuneyoshi. Expression of hepatocyte growth factor (HGF)/scatter factor and its receptor c-MET correlates with poor prognosis in synovial sarcoma. *Human Pathology.* Feb 2000. 31:2:185–192. DOI: 10.1016/S0046-8177(00)80218-X

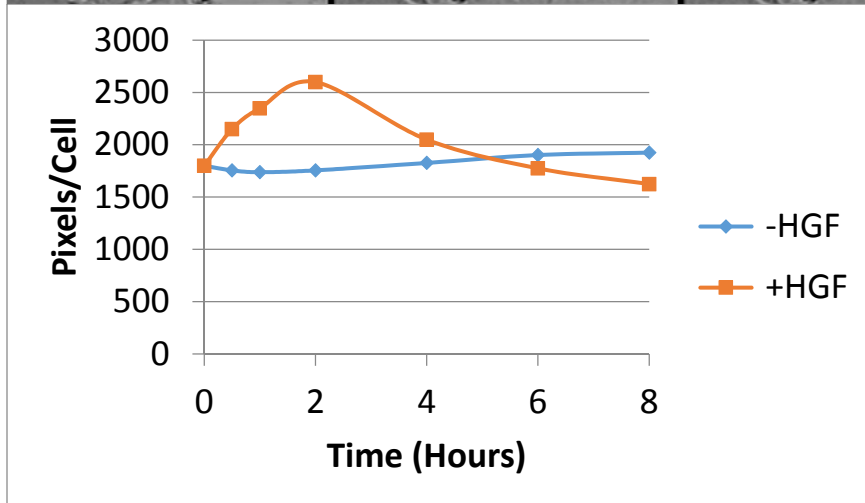
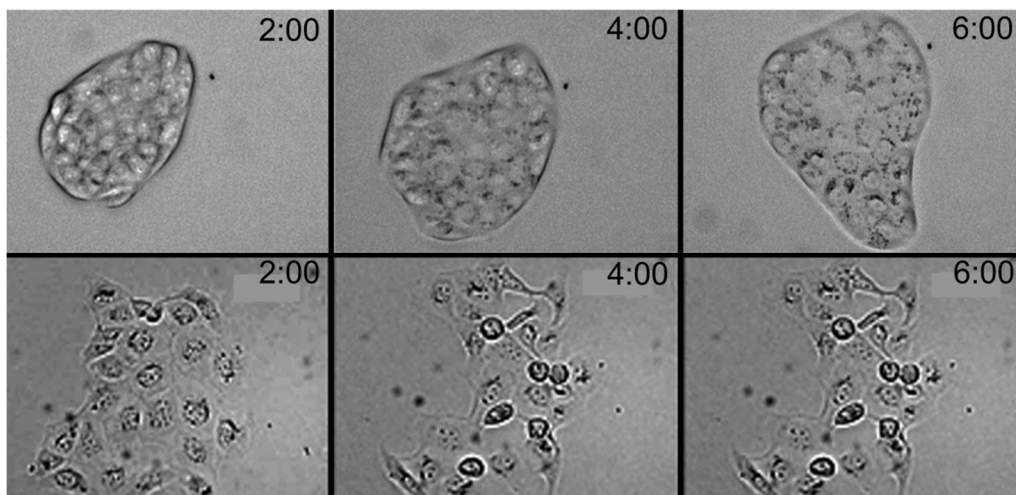
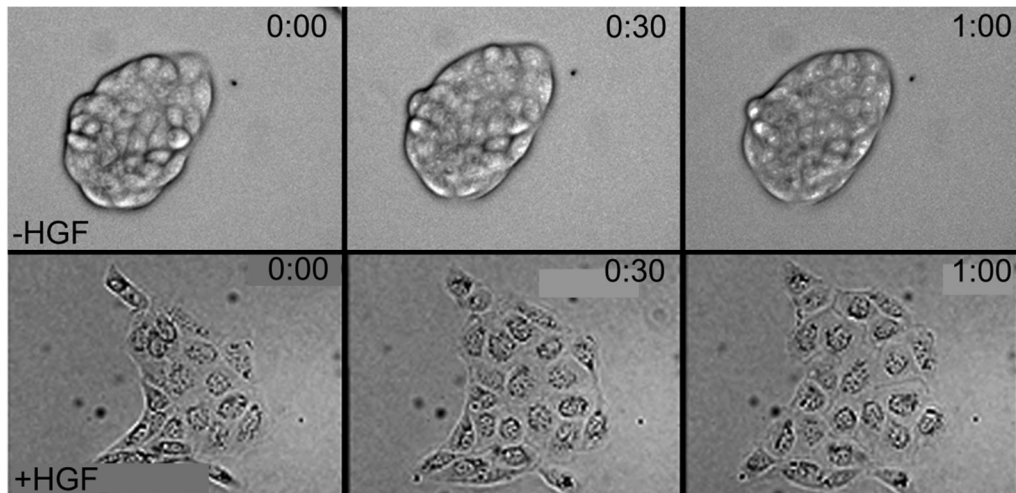


Figure 2.1: HGF-induced EMT Includes Phase of Cell Spreading, Followed by Phase of Cell Contraction. (A) MDCK cell time-lapse microscopy of +/-HGF treatment reveals cell scattering events. (B) Graph of cell surface area over time. HGF-treated cells increase surface area by 44% within first two hours, followed by cell contraction phase, when cells break cell-cell contacts and begin scattering.

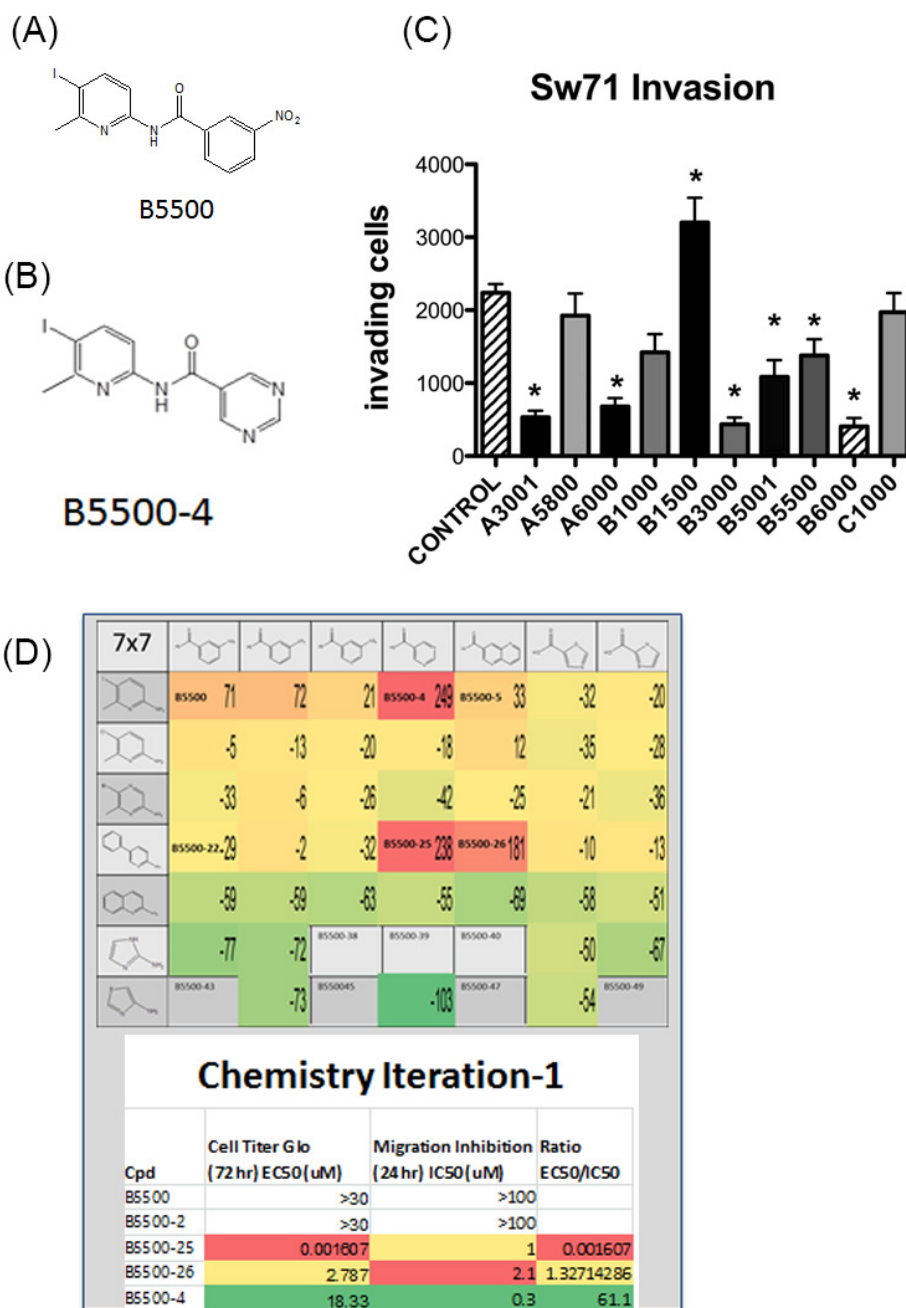


Figure 2.2: Characterization and Optimization of B5500. (A) Chemical structure of B5500. (B) Chemical structure of B5500-4. (C) SW71 cell invasion assay. SW71 cells were induced to invade through 3D collagen matrix onto a transwell membrane, towards 10% FBS chemoattractant. Tested compounds had final concentration of 10 uM. (D) Structure-activity relationship assay of B5500 and chemical derivatives. Left-side and right-side variations in the table axes represent chemical compound changes made to the B5500 scaffold. 49 derivatives were tested at a final concentration of 10 uM. Cell growth inhibition and migration inhibition of most potent compounds included in table.

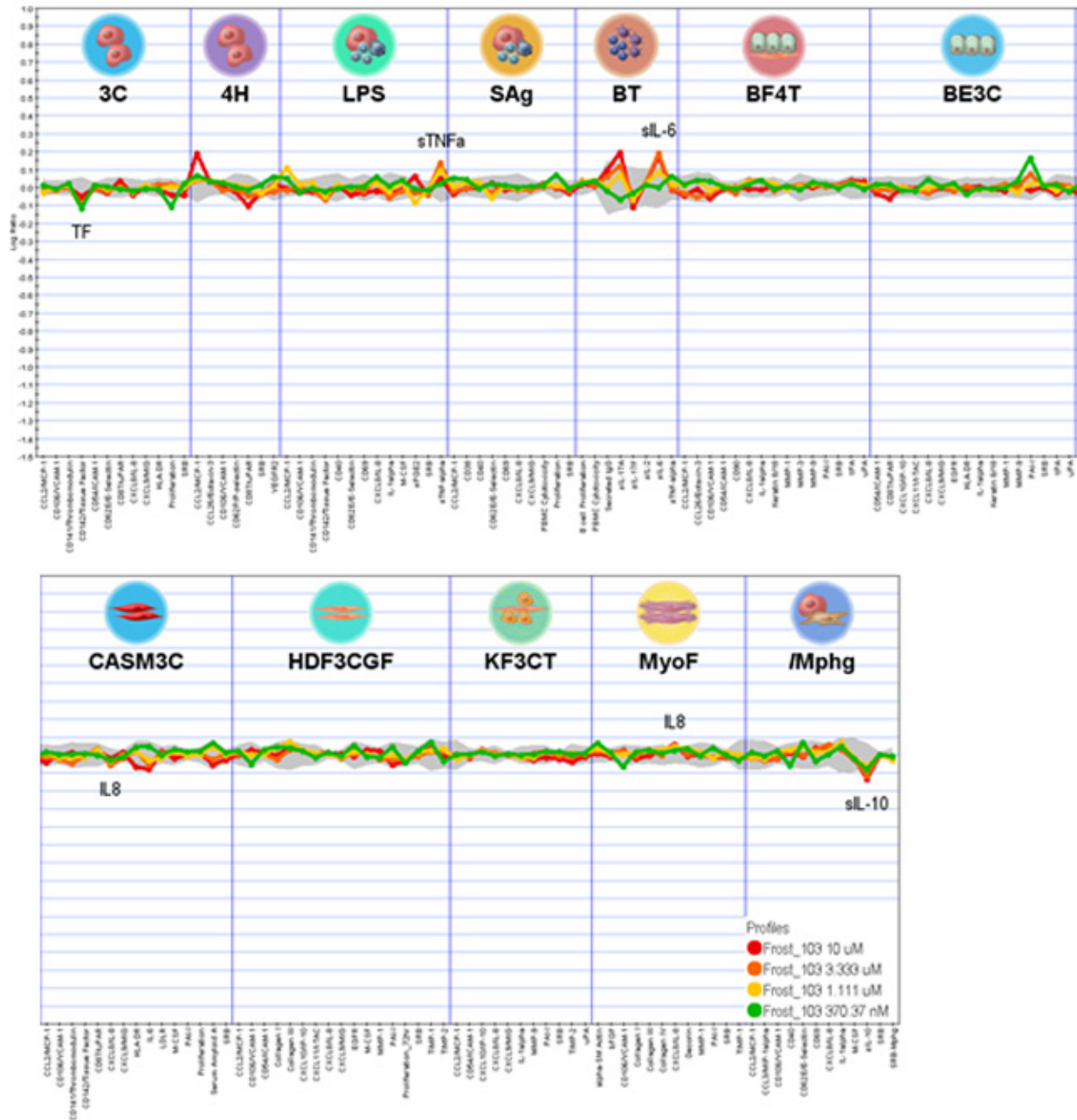


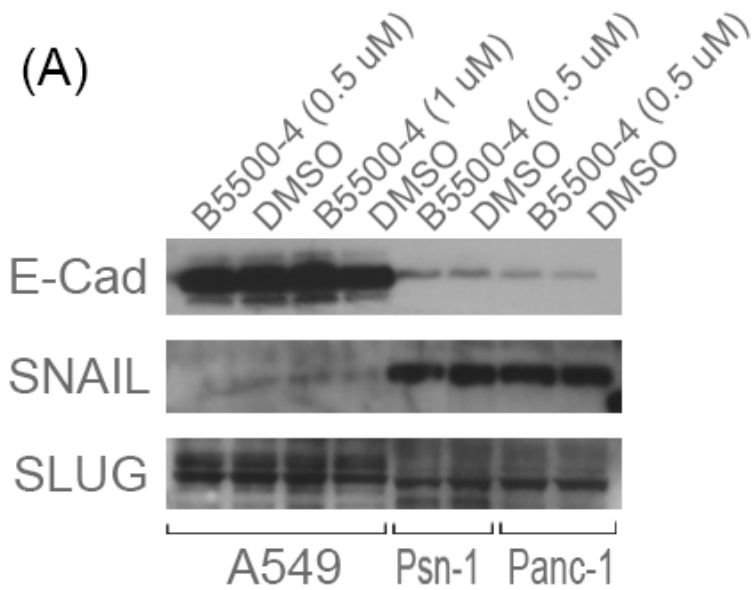
Figure 2.3: Inflammation Assay Reveals No Significant Change in Inflammatory Marker Expression. 12 cell lines were induced with B500-4 at several concentrations (10 uM, 3.33 uM, 1.11 uM, 37 nM) for 24 hrs and expression of a listed of inflammatory markers were measured. Markers revealed change beyond allowed standard error (gray zones) were noted to yield extremely small and insignificant changes from B500-4 treatment.

	B5500	B5500		B5500	B5500		B5500	B5500
Kinase	Data 1	Data 2	Kinase	Data 1	Data 2	Kinase	Data 1	Data 2
ABL1	97.65	99.50	CDK9/cyclinK	94.69	100.15	ERK1	86.61	91.88
ABL2/ARG	93.50	90.77	CDK9/cyclinT1	94.16	87.98	ERK2/MAPK1/P42MAPK	90.70	91.81
ACK1/TNK2	108.99	102.86	CHK1	97.77	98.03	FAK/PTK2	94.49	94.43
AKT1 (dPH, S473D)	94.40	90.01	CHK2	105.69	101.02	FER	96.77	96.84
AKT2/PKBb	98.55	89.04	CK1a1	99.32	98.82	FES/FPS	87.18	89.08
AKT3	96.51	92.20	CK1d	98.49	99.17	FGFR1	86.86	90.94
ALK	89.33	96.39	CK1e	82.07	73.89	FGFR2	85.46	88.35
ALK1/ACVRL1	101.44	96.99	CK1g1/CSNK1G1	96.79	101.28	FGFR3	80.20	83.45
ALK2/AVCR1	101.40	105.30	CK1g2	90.23	95.32	FGFR4	101.81	105.41
ALK4/ACVR1B	98.28	102.84	CK1g3/CSNK1G3	99.27	95.15	FGR	97.67	92.42
ALK5/TGFB-R1	96.09	102.90	CK2a	98.21	101.02	FLT1	99.20	102.61
ARAF	98.86	94.03	CK2a2	86.59	93.30	FLT3	97.80	91.23
ARK5	94.76	97.76	c-Kit	110.80	110.04	FLT4/VEGFR3	98.31	102.38
ASK1/MAP3K5	98.75	101.07	CLK1	101.37	102.44	FMS	91.96	101.84
Aurora A	99.11	98.31	CLK2	105.37	99.25	FRK/PTK5	99.78	95.41
Aurora B	101.38	95.45	CLK3	102.03	103.11	FYN	87.74	91.54
Aurora C/AURKC	83.05	74.92	CLK4	97.73	97.20	GCK/MAP4K2	95.89	95.79
AXL	110.42	104.53	c-MER	95.67	94.59	GRK2	101.36	96.07
BLK	100.43	101.14	c-MET	105.06	99.98	GRK3/ADRBK2	100.88	96.32
BMX	101.98	96.86	COT1/MAP3K8	84.60	87.52	GRK4	105.90	110.81
bRAF	101.19	100.97	CSK	103.20	103.13	GRK5	101.61	96.96
BRK	80.38	93.88	c-Src	98.52	100.88	GRK6	107.66	100.80
BRSK1	89.34	77.88	CTK/MATK/HYL	106.65	103.31	GRK7	91.96	96.22
BRSK2	99.12	95.65	DAPK1	90.49	82.24	GSK3a	95.53	105.38
BTK	99.88	93.39	DAPK2	102.18	103.95	GSK3b	98.43	95.64
CAMK1a	97.80	99.52	DCAMKL2	102.19	103.23	HCK	102.04	96.70
CAMK1b	103.20	100.58	DDR2	96.87	94.80	HGK/MAP4K4	92.86	96.85
CAMK1d	99.17	105.06	DMPK	106.49	105.65	HIPK1	99.32	104.99
CAMK1g	94.13	93.61	DRAK1/STK17A	101.54	86.00	HIPK2	100.73	102.77
CAMK2a	80.28	106.91	DYRK1/DYRK1A	100.84	103.58	HIPK3	104.70	102.51
CAMK2b	93.05	94.16	DYRK1B	106.10	100.12	HIPK4	102.93	97.51
CAMK4	88.30	86.72	DYRK2	86.59	94.71	IGF-1R	89.21	84.77
CAMKIId	84.70	80.79	DYRK3	99.13	99.84	IKK alpha/CHUK	82.63	80.16
CAMKIlg	90.17	95.12	DYRK4	88.08	95.54	IKK beta	100.72	90.15
CAMKK1	101.97	100.31	EGFR	98.69	96.48	IR	106.83	105.69
CAMKK2	93.94	99.24	EPHA1	97.41	95.05	IRAK1	101.71	97.17
CDK1 / cyclinA	100.83	102.23	EPHA2	87.95	90.57	IRAK4	99.95	104.84
CDK1/cyclin B	95.13	95.49	EPHA3	86.94	83.56	IRR/INSRR	97.85	95.42
CDK2 / cyclin A	74.35	76.46	EPHA4	91.82	101.72	ITK	100.66	105.18
CDK2 / cyclin E	94.46	95.20	EPHA5	91.34	97.77	JAK1	103.85	104.31
CDK3/cyclin E	91.36	96.61	EPHA7	85.98	85.40	JAK2	99.99	100.73
CDK4/cyclin D1	86.16	84.17	EPHA8	92.20	95.67	JAK2 (V617F)	83.30	88.15
CDK4/cyclin D3	103.83	94.22	EPHB1	97.07	97.38	JAK3	103.70	96.86
CDK5/p25	100.39	96.82	EPHB2	102.72	100.14	JNK1a1	102.21	103.52
CDK5/p35	74.72	63.90	EPHB3	94.14	95.92	JNK2a2	104.78	102.98
CDK6/cyclin D1	92.89	94.76	EPHB4	94.78	95.92	JNK3	97.11	102.06
CDK6/cyclin D3	92.27	93.60	ErbB2/HER2	91.94	98.81	KDR/VEGFR2	91.86	95.81
CDK7/cyclinH/MNAT1	103.81	110.78	ErbB4/HER4	94.85	99.13	KHS/MAP4K5	85.38	88.90

Figure 2.4: Kinase Screen of B5500 Does Not Block Kinases in Kinase Screen. B5500 was tested for effects on activity levels of a total of 230 kinases. Raw scores were generated from screen data, with 100 indicating a 100% normal level of kinase activity. B5500 does not significantly alter any of the 230 kinases screened.

	B5500	B5500		B5500	B5500		B5500	B5500
Kinase	Data 1	Data 2	Kinase	Data 1	Data 2	Kinase	Data 1	Data 2
LCK	81.83	83.92	P38b	98.30	101.39	RIPK5	101.65	102.50
LIMK1	97.88	97.78	P38d/MAPK13	93.99	101.67	ROCK1	88.86	95.51
LKB1	113.17	113.00	P38g/MAPK12	105.49	88.01	ROCK2/ROKα	89.93	96.58
LOK/STK10	98.00	97.69	p70S6K	96.77	101.24	RON/MST1R	100.17	97.90
LRRK2	101.30	92.98	p70S6Kb /RPS6KB2	103.54	107.66	ROS/ROS1	88.59	92.53
LYN	86.52	93.47	PAK1	103.55	104.14	RSK1	97.19	95.08
LYN B	101.45	98.40	PAK2	85.80	86.84	RSK2	89.39	88.15
MAPKAPK2	97.71	94.97	PAK3	101.50	92.13	RSK3	97.18	97.45
MAPKAPK3	97.38	100.19	PAK4	93.44	101.28	RSK4/RPS6KA6	95.01	97.96
MAPKAPK5/PRAK	101.04	83.30	PAK5	82.54	80.16	SGK1 (d1-59, S422D)	93.44	99.12
MARK1	105.14	99.80	PAK6	103.05	102.90	SGK2	97.82	100.40
MARK2	101.41	101.93	PASK	101.81	94.33	SGK3/SGKL	100.65	101.92
MARK3	93.24	93.89	PBK/TOPK	98.43	96.65	SIK2/SNF1LK2/QIK	131.98	136.34
MARK4	101.78	100.16	PDGFRα	82.10	89.54	SLK/STK2	89.12	73.40
MEK1	98.00	100.83	PDGFRβ	81.16	81.21	SNARK/NUAK2	100.41	102.26
MEK2	103.77	107.98	PDK1/PDPK1	99.71	98.75	SRMS	101.20	102.37
MEKK2	104.48	109.34	PHKg1	95.59	100.86	SRPK1	88.43	88.21
MEKK3	102.66	96.03	PHKg2	91.19	88.64	SRPK2	75.77	76.86
MELK	84.86	90.00	PIM1	95.99	95.78	STK16	96.98	89.70
MINK/MINK1	100.12	100.88	PIM2	90.08	88.17	STK22D	105.66	95.16
MKK6	105.04	109.63	PIM3	85.58	87.62	STK25/YSK1	91.52	98.49
MLCK/MYLK	89.80	91.15	PKA	99.13	95.23	STK33	95.74	98.54
MLCK2/MYLK2	102.59	92.43	PKC μ	101.46	107.15	SYK	109.28	104.87
MLK1/MAP3K9	93.68	103.89	PKC ν	104.21	99.77	TAK1/TAB1/MAP3K7	98.39	98.21
MLK2/MAP3K10	106.45	107.61	PKCα	91.15	86.12	TAOK1	97.40	97.06
MLK3/MAP3K11	103.35	100.65	PKCβI	93.65	96.22	TAOK2/TAO1	89.05	98.23
MNK2	103.87	103.38	PKCβII	99.70	99.00	TAOK3/JIK	102.61	109.22
MRCKα/CDC42BPA	90.10	94.67	PKCδ	86.73	90.26	TBK1	115.71	115.69
MRCKβ/CDC42BPB	103.68	100.27	PKCε	90.41	91.34	TEC	94.11	89.33
MSK1/RPS6KA5	82.26	88.07	PKCεeta	103.09	104.26	TGFβR2	100.67	101.60
MSK2/RPS6KA4	98.59	98.30	PKCγ	99.79	96.48	TIE2/TEK	97.74	95.91
MSSK1/STK23	93.70	95.12	PKCιota	94.66	99.13	TRKA/NTRK1	92.70	81.77
MST1/STK4	107.35	98.63	PKCθeta	98.05	98.13	TRKB/NTRK2	76.12	80.32
MST2/STK3	114.53	100.49	PKCzeta	90.90	96.24	TRKC	94.26	93.30
MST3/STK24	104.11	106.30	PKD2 / PRKD2	97.57	94.90	TSSK2	95.74	95.19
MST4	99.97	102.59	PKG1 α	94.02	99.85	TTK	99.58	103.98
MUSK	104.65	97.81	PKG1b	102.42	105.94	TXK	109.17	109.38
NEK1	104.12	104.40	PKG2/PRKG2	81.31	83.32	TYK1/LTK	115.43	113.29
NEK11	94.66	101.78	PKN1/PRK1	98.17	97.67	TYK2	98.26	100.27
NEK2	108.46	100.26	PKN2/PRK2	99.55	95.55	TYRO3/SKY	88.18	90.03
NEK3	148.21	132.42	PLK1	100.69	103.62	VRK1	100.49	92.03
NEK4	104.12	101.75	PLK2	107.23	98.78	Wee1	92.31	92.97
NEK6	155.50	138.84	PLK3	102.27	100.91	WNK2	101.64	107.53
NEK7	100.61	99.50	PRKX	96.48	99.87	WNK3	97.89	107.83
NEK9	97.81	102.11	PYK2/PTK2B/FAK2	83.92	80.63	YES	99.95	99.54
NIK/MAP3K14	83.20	96.29	RAF1	97.88	102.25	ZAK	99.42	105.23
NLK	90.72	98.61	RET	81.22	84.09	ZAP70	100.91	97.89
P38a	101.44	94.15	RIPK2	106.84	108.32	ZIPK/DAPK3	97.25	104.80

Figure 2.4 (continued): Kinase Screen of B5500 Does Not Block Kinases in Kinase Screen. B5500 was tested for effects on activity levels of a total of 230 kinases. Raw scores were generated from screen data, with 100 indicating a 100% normal level of kinase activity. B5500 does not significantly alter any of the 230 kinases screened.



(B) B5500-4 Invasion Assay

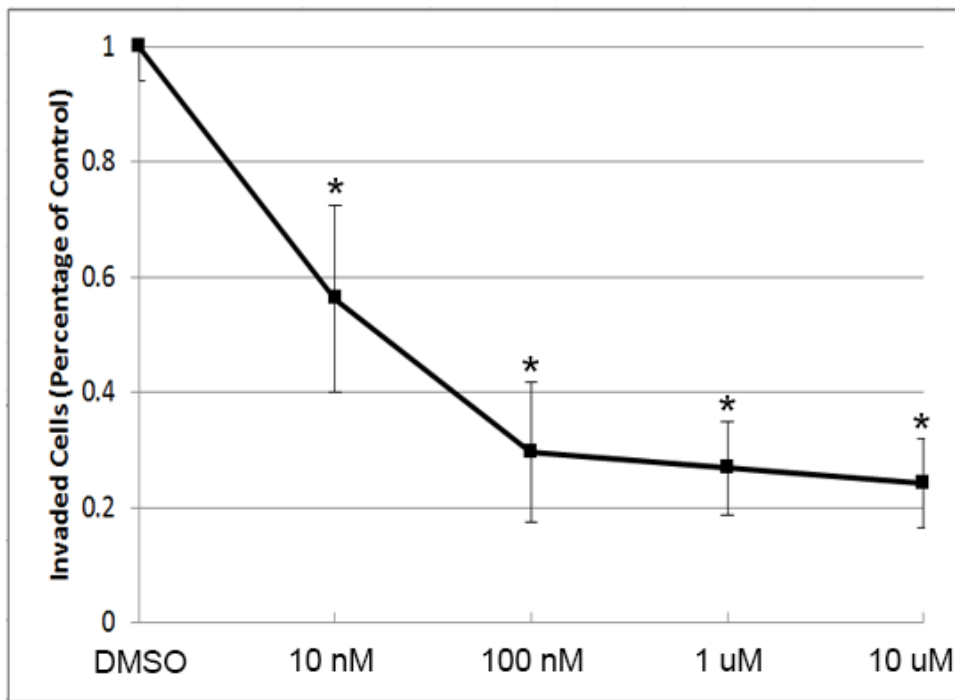
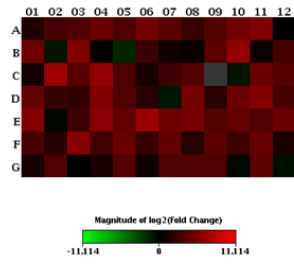


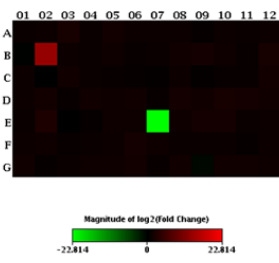
Figure 2.5: B5500-4 Does Not Alter Levels of Classic EMT Markers. (A) Western blot of EMT markers in human cancer cell lines with addition of B5500-4 or DMSO. A549, Psn-1 and Panc-1 cell lines were tested for changes in expression in e-Cadherin, SLUG, and Snail. (B) SW71 cell invasion assay of B5500-4. Dosage curve yielded IC-50 of ~27 nM.

(A) Visualization of log₂(Fold Change)



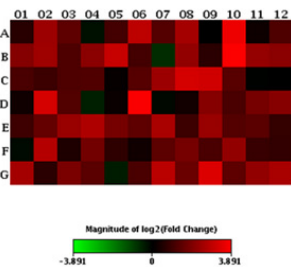
Layout	01	02	03	04	05	06	07	08	09	10	11	12
A	AKT1	AKT1S1	AKT2	AKT3	CAB39	CAB39L	CDC42	CHUK	DDIT4	DDIT4L	DEPTOR	EIF4B
	2.75	8.92	11.53	25.73	11.02	35.99	15.43	5.35	12.02	32.26	52.30	1.01
B	EIF4E	EIF4EBP1	EIF4EBP2	FKBP1A	FKBP8	GSK3B	HIF1A	HRAS	HSPA4	IGF1	IGFBP3	IKKBK
	29.32	-1.90	52.24	-1.09	-3.20	5.80	1.63	1.28	15.53	85.04	1.54	8.40
C	ILK	INS	INSR	IRS1	MAPK1	MAPK3	MAPKAP1	MLST8	MTOR	MYO1C	PDRK1	PIK3C3
	1.79	116.60	13.81	92.19	9.83	2.10	7.08	11.56	-2216.10	-1.85	24.57	13.61
D	PIK3CA	PIK3CB	PIK3CD	PIK3CG	PLD1	PLD2	PPP2CA	PPP2R2B	PPP2R4	PRKAA1	PRKAA2	PRKAB1
	20.13	5.13	4.21	53.58	10.76	3.26	-1.91	33.44	3.05	26.53	53.05	8.10
E	PRKAB2	PRKAG1	PRKAG2	PRKAG3	PRKCA	PRKCB	PRKCE	PRKCG	PTEN	RHEB	RHOA	RICTOR
	53.44	-1.22	5.98	67.37	18.55	110.40	28.93	36.76	12.13	20.11	11.46	22.86
F	RP56	RP56K1	RP56K2	RP56K4	RP56K6	RP56K8	RPTOR	RRAG	RRAGB	RRAGC	RRAGD	SGK1
	8.20	3.12	57.38	7.27	23.72	4.89	18.28	3.03	16.08	6.46	22.31	2.38
G	STK11	STRADB	TELO2	TP53	TSC1	TSC2	ULK1	ULK2	VEGFA	VEGFB	VEGFC	YWHQA
	2.18	10.25	-1.04	2.07	12.62	1.61	9.77	10.45	10.48	-1.39	17.06	-1.65

(B) Visualization of log₂(Fold Change)



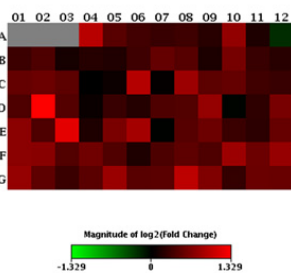
Layout	01	02	03	04	05	06	07	08	09	10	11	12
A	ADAMTS1	ADAMTS13	ADAMTS8	CD44	CDH1	CLEC3B	CNTN1	COL11A1	COL12A1	COL14A1	COL15A1	COL16A1
	1.86	2.13	3.88	1.82	2.90	2.02	2.01	1.98	1.52	2.19	1.87	2.00
B	COL1A1	COL4A2	COL5A1	COL6A1	COL6A2	COL7A1	COL8A1	CTGF	CTNNA1	CTNNA2	CTNND1	CTNND2
	-1.07	10337.80	2.02	1.91	2.27	1.64	1.91	2.85	3.44	2.45	1.54	3.98
C	ECM1	FN1	HAS1	ICAM1	ITGA1	ITGA2	ITGA3	ITGA4	ITGA5	ITGA6	ITGA7	ITGA8
	1.98	1.02	2.69	1.86	1.67	1.45	1.29	2.03	1.33	1.57	1.60	3.22
D	ITGAL	ITGAM	ITGAV	ITGB1	ITGB2	ITGB3	ITGB4	ITGB5	KAL1	LAMA1	LAMA2	LAMA3
	2.05	2.95	1.60	2.77	2.24	2.57	1.71	3.39	2.86	3.80	3.47	2.60
E	LAMB1	LAMB3	LAMC1	MMP1	MMP10	MMP11	MMP12	MMP13	MMP14	MMP15	MMP16	MMP2
	1.97	5.81	1.02	1.51	2.40	2.34	-7374760.71	2.25	3.63	3.67	1.92	2.17
F	MMP3	MMP7	MMP8	MMP9	NCAM1	PECAM1	SELE	SELL	SELP	SGCE	SPARC	SPG7
	2.06	2.31	1.70	1.76	2.22	3.40	2.46	1.90	1.81	1.95	1.44	2.06
G	SPP1	TGFB1	THBS1	THBS2	THBS3	TIMP1	TIMP2	TIMP3	TNC	VCAM1	VCAN	VTN

(C) Visualization of log₂(Fold Change)



Layout	01	02	03	04	05	06	07	08	09	10	11	12
A	AHNAK	AKT1	BMP1	BMP2	BMP7	CALD1	CAMK2N1	CAV2	CDH1	CDH2	COL1A2	COL3A1
	1.52	5.34	2.68	-1.19	2.07	7.39	2.43	2.77	1.01	12.67	1.15	2.26
B	COL5A2	CTNNA1	DSC2	DSP	EGFR	ERBB3	ESR1	F1R	FGFR1	FN1	FOXO2	FZD7
	4.15	5.39	2.28	4.43	8.22	2.05	-1.58	4.77	1.56	14.84	4.89	4.35
C	GNG11	GSC	GSK3B	IGFBP4	IL1RN	ILK	ITGA5	ITGAV	ITGB1	JAG1	KRT14	KRT19
	2.17	1.90	2.29	2.31	1.07	2.49	5.26	9.60	9.23	2.51	-1.03	1.01
D	KRT7	MAP1B	MMP2	MMP3	MMP9	MSH1	MST1R	NODAL	NOTCH1	NUDT13	OCLN	PDGFRB
	1.18	9.60	2.38	-1.37	1.11	14.26	-1.08	1.21	4.18	2.19	3.52	4.20
E	PLEK2	DES1	PTK2	PTPAA1	RAC1	RGS2	SERPINE1	GEMIN2	SMAD2	SNAI1	SNAI2	SNAI3
	1.92	2.85	5.08	6.47	3.51	2.69	6.03	1.87	5.15	2.43	2.59	1.74
F	SOX10	SPARC	SPP1	STAT3	STEAP1	TCF3	TCF4	TFF12	TGFB1	TGFB2	TGFB3	TIMP1
	-1.11	6.91	1.37	3.37	1.62	1.19	2.66	3.46	2.19	4.78	1.82	1.69
G	TMEFF1	TMEM132A	TSPAN13	TWIST1	VCAN	VIM	VPS13A	WNT1	WNT5A	WNT5B	ZEB1	ZEB2
	5.73	1.57	3.67	2.60	-1.34	2.20	7.23	3.09	10.43	2.68	4.80	0.80

(D) Visualization of log₂(Fold Change)



Layout	01	02	03	04	05	06	07	08	09	10	11	12
A	ACTR2	ACTR3	ARAP1	ARFP2	ARHGAP6	ARHGDB8	ARHGEP1	ARPC18	ARPC2	ARPC3	ARPC4	ARPC5
	-1.82	-1.82	-1.82	1.97	1.38	1.27	1.23	1.25	1.16	1.71	1.11	-1.17
B	AURKA	AURKB	BAIAP2	CALD1	CALM1	CASK	CCNA1	CCNB2	CDC42	CDC42BP1	CDC42BP2	
	1.24	1.33	1.08	1.15	1.12	1.25	1.43	1.36	1.10	1.54	1.23	1.15
C	CDC42EP3	CDK5	CDK5R1	CFL1	CIT	CLASP1	CLASP2	CLP1	CLP2	CRK	CTTN	CYFIP1
	1.43	1.48	1.39	-1.00	1.04	1.93	1.02	1.77	1.39	1.43	1.26	1.23
D	CYFIP2	DIAPH1	DSTN	EZR	FNBP1L	FSCN2	GSN	IQGAP1	IQGAP2	LMK1	LMK2	LLGL1
	1.32	2.51	1.36	1.03	1.22	1.14	1.32	1.34	1.72	-1.01	1.18	1.55
E	MACF1	MAP3K11	MAP4	MAPK13	MAPRE1	MAPRE2	MAPT	MARK2	MID1	MSN	MYLK	MYLK2
	1.66	1.32	2.29	1.12	1.55	1.82	-1.01	1.37	1.48	1.23	1.18	1.44
F	NCK1	NCK2	PAK1	PAK4	PFN2	PHLDB2	PKFYVE	PPP1R12A	PPP1R12B	PPP3CA	PPP3CB	RAC1
	1.66	1.64	1.34	1.49	1.34	1.12	1.32	1.40	1.32	1.77	1.48	1.73
G	RACGAP1	RDX	RHOA	ROCK1	SSH1	SSH2	STH1	TIAM1	VASP	WAS	WASP1	WASL
	1.72	1.41	1.24	1.39	1.75	1.38	1.39	1.99	1.59	1.21	1.47	1.46

Figure 2.6: qPCR Array Results Indicate Fold-increase of Select Genes. Genes related to (A) EMT, (B) ECM (C) cytoskeleton, and (D) mTOR pathway were tested. mRNA from SW71 cells induced with either DMSO or B5500-4 (10 uM) vcan for 24 hrs was extracted, converted to cDNA, and run through qPCR assay. Genes of significant change include Col4A2 (1.05x10⁴ fold change), MMP12 (-7.37x10⁶ fold change), and mTOR (-2.22x10³ fold change).

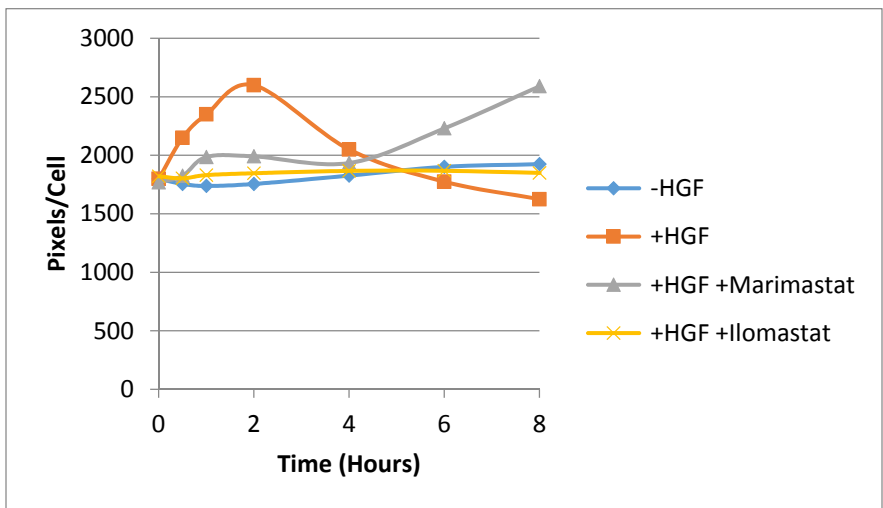
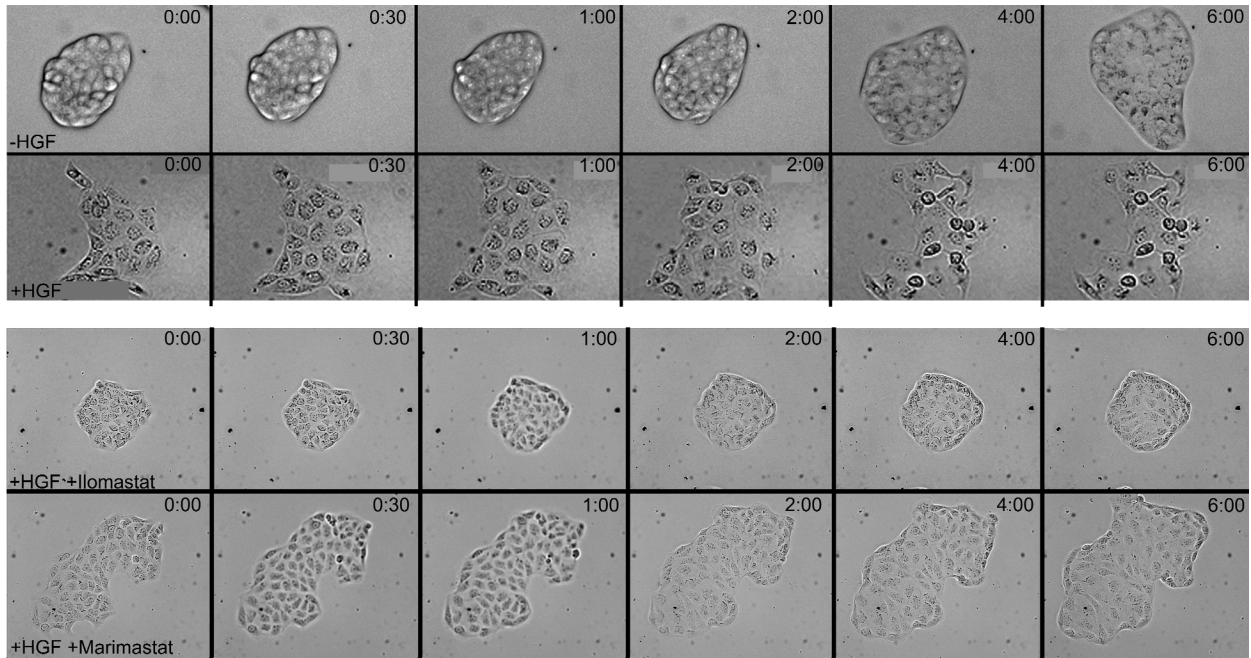


Figure 2.7: MMP-9 is Required for HGF-induced Epithelial Cell Scattering, and MMP-12 is Required for HGF-induced Cell Contraction Phase of Epithelial Cell Scattering. (A) MDCK time-lapse microscopy with HGF and Ilomastat (MMP-9) reveals failure of HGF-induced cell scattering. (B) MDCK time-lapse microscopy with HGF and Marimastat (MMP-12) shows MMP-12 role in HGF-induced cell contraction as a part of the cell scattering program. (C) MDCK cell surface area changes over time.

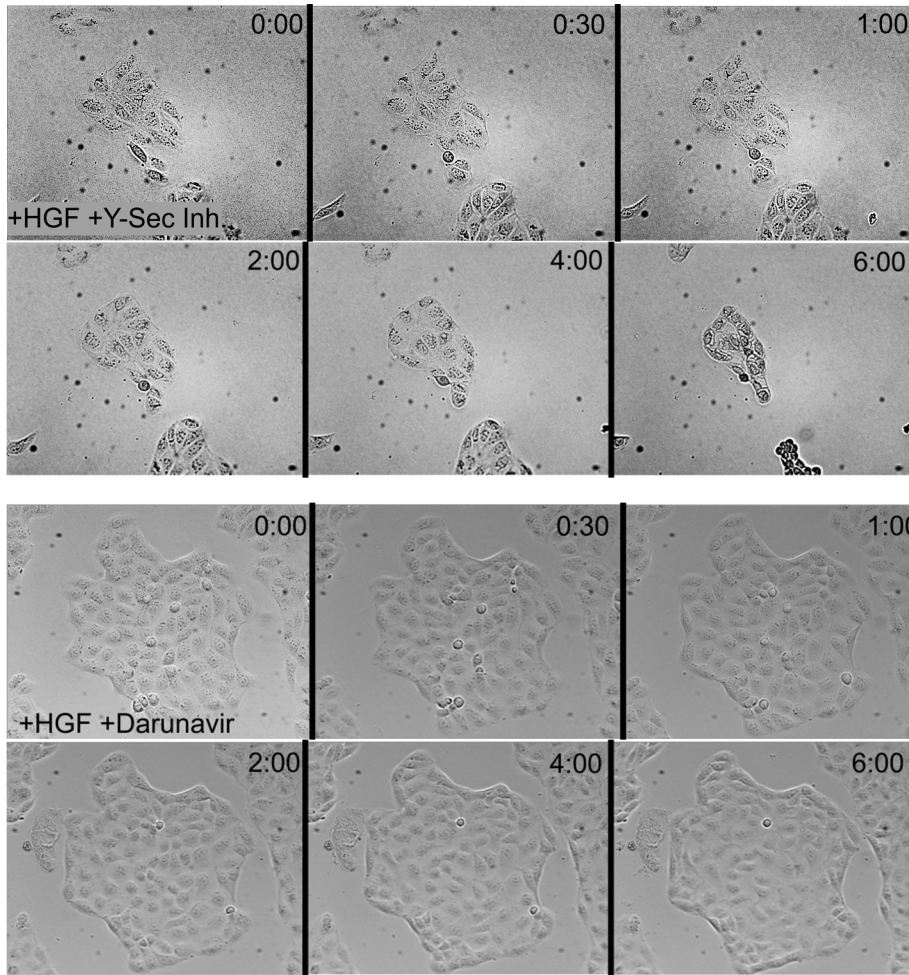


Figure 2.8: Furin Inhibition Blocks HGF-induced EMT; Y-Sec Inhibition is Cytotoxic. (A) MDCK cell time-lapse microscopy with HGF and Y-Secretase inhibitor reveals quick cell death by as early as 6 hours after treatment. (B) MDCK cell time-lapse microscopy with HGF and Darunavir (furin inhibitor) reveals failure of epithelial cell scattering.

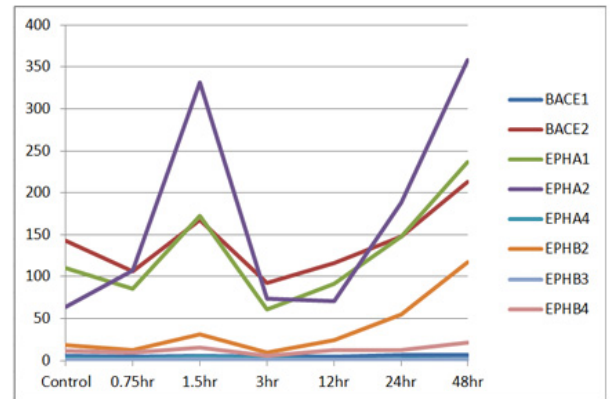
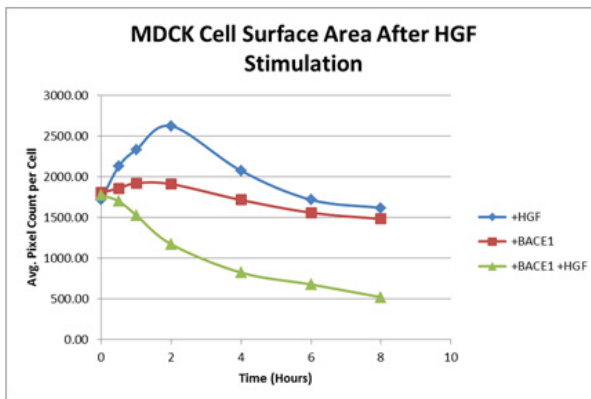
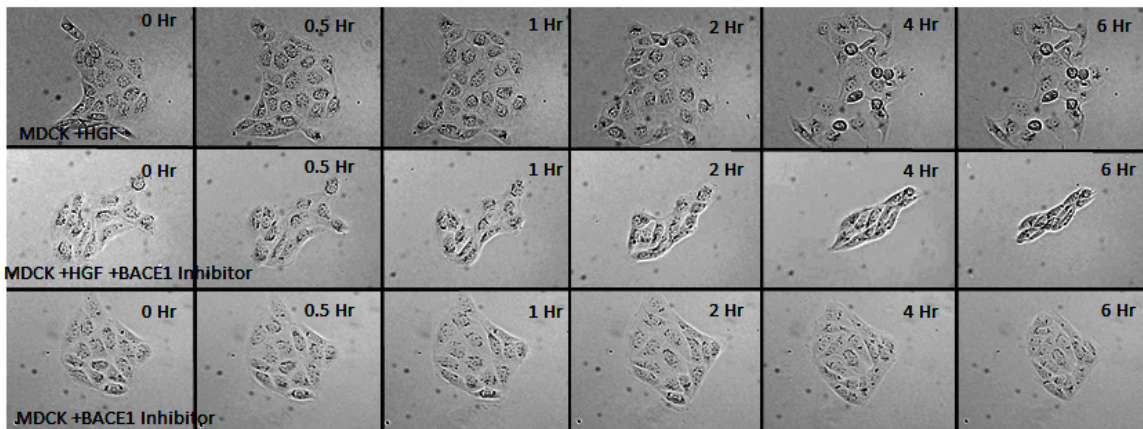


Figure 2.9: BACE is Required for Early EMT Cell Spreading. (A) Time-lapse live cell microscopy of MDCK cells were filmed over 6 hrs after induced with HGF and/or BACE inhibitor. (B) MDCK cell surface area chart illustrates the change in cell spreading/cell compaction during HGF induction. (C) Changes in gene expression of Eph family genes and BACE family genes at different time points after HGF induction.

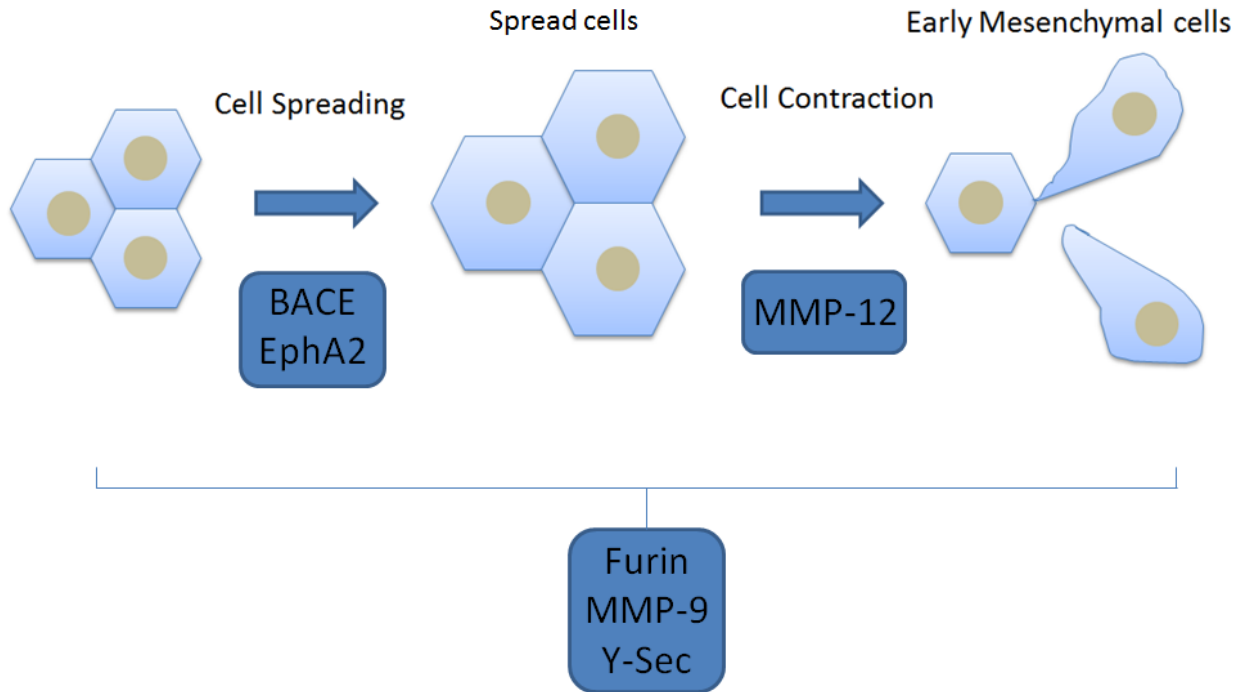


Figure 2.10: Model for Proteolytic Activity during Early EMT Events. A two-phase characterization of epithelial cell scattering includes cell spreading followed by cell contraction, which is when cell-cell contacts are broken. BACE activity is required for cell spreading to progress, while MMP-12 activity is required for cell contraction. Furin and MMP-9 are both required for cell scattering to progress, blocking both spreading and contraction phases. Y-Sec activity is required for cell survival and may not necessarily be involved in the c-Met pathway.

Jeffrey T. Schuler
730 E 700 N
Provo, UT, 84606
801-857-7028
jeffrey.t.schuler@gmail.com

EDUCATION

Brigham Young University	Sep 2006-Dec 2014
BS in Physiology and Developmental Biology	
BS in Business Management: General Management Emphasis	GPA: 3.3
MS in Physiology and Developmental Biology	GPA: 3.7

WORK EXPERIENCE

Undergraduate Researcher	Aug 2009- Aug 2010
McKay School of Education: Brigham Young University	

Mentored under Dr. Ellen Williams and Dr. Joseph Matthews. Used analytical software (NVivo & Minitab) to characterize properties of school districts as effective professional learning communities.

Teacher's Aide: Biology 100	Aug 2010-Apr 2012
Biology Department: College of Life Sciences: Brigham Young University	

Under Dr. Melinda Ostraff, regularly led class lectures, mentored peers, and evaluated student performance. Developed new lecture presentations incorporating new course material; lecture topics covered basic biological concepts, including cell theory, mitosis/meiosis, Mendelian genetics, evolution, and ecology.

Undergraduate/Graduate Researcher	Apr 2010- present
PDBio Department: College of Life Sciences: Brigham Young University	

Mentored under Dr. Marc Hansen. Group leader over biochemistry experiments. Characterized cell-cell junction proteins in epithelia under dynamic conditions, and molecular targets of small chemical inhibitors of Epithelial-Mesenchymal Transition (EMT) and Cancer Metastasis. Findings published in the Journal of Biochemical and Biophysical Research Communications and Journal of Experimental Cell Research.

Leader of Senior Research Capstone Project. Tested potential anti-cancer drug compounds through several well-established drug development tests, including NCI-60 growth assays, EMT assays, toxicity studies, and pharmacokinetics/pharmacodynamics studies.

Chemical compounds to be licensed to IMD for clinical trials testing and submission for FDA approval.

Master's Thesis work on characterizing mechanism of action for potential anti-metastatic compound (B5500-4). Studies and experiments include techniques in immunofluorescent microscopy, time-lapse microscopy, western blot, ELISA, invasion assays, EMT assays, qPCR, and RNA-seq.

Course Team Instructor: Principles of Biology (PDBio 120) Jan 2013-Apr 2013
PDBio Department: College of Life Sciences: Brigham Young University

Team-taught PDBio 120 course with Dr. Juan Arroyo. Taught every other class lecture, co-wrote weekly exam questions, graded course material, mentored students during office hours, and coordinated undergraduate TA responsibilities and work.

Course Instructor: Advanced Physiology Lab Aug 2012-present
PDBio Department: College of Life Sciences: Brigham Young University

Led 3-hour weekly laboratory course in Advanced Physiology (PDBio 363). Taught mini-lecture at start of class, mentored students during class and office hours, graded lab reports, and held test reviews.

SERVICE

Hospital Volunteer Sep 2010- Jan 2013
Utah Valley Regional Medical Center: ER Trauma Center

Transported patients, medical equipment, and supplies to and from the ER. Regularly interacted with patients, doctors, and other medical staff.

Missionary Service Aug 2007- Aug 2009
The Church of Jesus Christ of Latter-day Saints

Served a two year, non-profit mission in Michigan. Invited others to learn more about religious beliefs. Also provided service to individuals and community organizations. Led and supervised 20-30 peers.

AWARDS

Cancer Research Center Summer Fellowship Apr 2011
Brigham Young University Cancer Research Center

Awarded research grant for independent research project on the study novel small chemical inhibitors of tumor metastases. Tested structure-activity relationship of potential anti-cancer drug derivatives.

FUNDING

Teacher's Aide Funding: Department of Physiology and Dev. Biology

Sep 2012-Apr 2014

PUBLICATIONS

Call GS, Hansen MDH, et al. A zyxin-nectin interaction facilitates zyxin localization to cell-cell adhesions. *Biochemical and Biophysical Research Communications*. 2011 Nov 25;415(3):485-9. doi: 10.1016/j.bbrc.2011.10.099. Epub 2011 Oct 28.

Hoj JP, Hansen MDH, et al. Cellular contractility changes are sufficient to drive epithelial scattering. *Experimental Cell Research*. 2014 Apr 26. pii: S0014-4827(14)00169-4. doi: 10.1016/j.yexcr.2014.04.011.

PRESENTATIONS AND ABSTRACTS

Schuler JT, and Hansen MDH. Characterizing small chemical inhibitors of c-Met-induced EMT. BYU Cancer Research Center Summer Fellowship Oral Presentation. August 2011.

Schuler JT, Hansen MDH, et al. IND-enabling studies of B3000 and A5000. BYU Senior Capstone Competition Oral Presentation. April 2012.

Schuler JT, Hansen MDH, et al. Anti-cancer Drug Development Process. BYU Scientific Poster Miniconference. March 2012.

REFERENCES

Dr. Marc Hansen
Professor, College of Life Sciences
Brigham Young University
587 WIDB
Provo, UT, 84602
(801)422-4998
marchansen@byu.edu

Dr. Juan Arroyo
Professor, College of Life Sciences
Brigham Young University
597 WIDB
Provo, UT, 84602
(801)422-3221
jarroyo@byu.edu

Dr. Ellen Williams
Professor, McKay College of Education
Brigham Young University
3114 MCKB
Provo, UT, 84602
(801)422-5135
ellenwilliams@byu.edu